1994-03

Improving transient signal synthesis through noise modeling and noise removal

Frack, Kenneth L., Jr.

Monterey, California. Naval Postgraduate School

NAVAL POSTGRADUATE SCHOOL
Monterey, California

THESIS

IMPROVING TRANSIENT SIGNAL SYNTHESIS THROUGH NOISE MODELING AND NOISE REMOVAL

by

Kenneth L. Frack, Jr.

March, 1994

Thesis Advisor: Charles W. Therrien

REPORT DOCUMENTATION PAGE

1a. REPORT SECURITY CLASSIFICATION UNCLASSIFIED	1b. RESTRICTIVE MARKINGS
2a. SECURITY CLASSIFICATION AUTHORITY	3. DISTRIBUTION/AVAILABILITY OF REPORT Approved for public release; distribution is unlimited.
2b. DECLASSIFICATION/DOWNGRADING SCHEDULE	
4. PERFORMING ORGANIZATION REPORT NUMBER(S)	5. MONITORING ORGANIZATION REPORT NUMBER(S)
6a. NAME OF PERFORMING ORGANIZATION Electrical Engineering Dept. Naval Postgraduate School 6b. OFFICE SYMBOL (*if applicable*) EC	7a. NAME OF MONITORING ORGANIZATION Naval Postgraduate School
6c. ADDRESS (*City, State, and ZIP Code*) Monterey, CA 93943	7b. ADDRESS (*City, State, and ZIP Code*) Monterey, CA 93943
8a. NAME OF FUNDING/SPONSORING ORGANIZATION 8b. OFFICE SYMBOL (*if applicable*)	9. PROCUREMENT INSTRUMENT IDENTIFICATION NUMBER
8c. ADDRESS (*City, State, and ZIP Code*)	10. SOURCE OF FUNDING NUMBERS PROGRAM ELEMENT NO. / PROJECT NO. / TASK NO. / WORK UNIT ACCESSION NO.

11. TITLE (*Include Security Classification*) IMPROVING TRANSIENT SIGNAL SYNTHESIS THROUGH NOISE MODELING AND NOISE REMOVAL

12. PERSONAL AUTHOR(S)
Frack, Kenneth Lawrence, Jr.

13a. TYPE OF REPORT	13b. TIME COVERED	14. DATE OF REPORT (*Year, Month, Day*)	15. PAGE COUNT
Master's Thesis	FROM 01/93 TO 3/94	March 1994	70

16. SUPPLEMENTARY NOTATION The views expressed in this thesis are those of the author and do not reflect the official policy or position of the Department of Defense or the United States Government.

17. COSATI CODES			18. SUBJECT TERMS (*Continue on reverse if necessary and identify by block number*)
FIELD	GROUP	SUB-GROUP	AR Modeling. MA Modeling ARMA Modeling. Noise. Noise Modeling. Short-time Wiener Filter. Wiener Filter. Noise Removal

19. ABSTRACT (*Continue on reverse if necessary and identify by block number*)

This thesis examines signal modeling techniques and their application to ambient ocean noise for purposes of noise removal and for generating realistic synthetic noise to add to synthetically generated transient signals. Higher order statistics of the noise are examined to test for Gaussianity. Stochastic approaches to AR, MA, and ARMA modeling are compared to see which technique yields the "best" synthetic noise. Results from the modeling process are used to develop a short-time Wiener filter which can be used to condition a real signal for further processing through effective noise removal.

20. DISTRIBUTION/AVAILABILITY OF ABSTRACT ☒ UNCLASSIFIED/UNLIMITED ☐ SAME AS RPT. ☐ DTIC USERS	21. ABSTRACT SECURITY CLASSIFICATION UNCLASSIFIED
22a. NAME OF RESPONSIBLE INDIVIDUAL Charles W. Therrien	22b. TELEPHONE (*Include Area Code*) (408) 656-3347 22c. OFFICE SYMBOL EC/Ti

Approved for public release; distribution is unlimited.

IMPROVING TRANSIENT SIGNAL SYNTHESIS THROUGH NOISE MODELING AND NOISE REMOVAL

by

Kenneth L. Frack, Jr.
Lieutenant, United States Navy
B.S., United States Naval Academy, 1987

Submitted in partial fulfillment of the
requirements for the degree of

MASTER OF SCIENCE IN ELECTRICAL ENGINEERING

from the

NAVAL POSTGRADUATE SCHOOL

March, 1994

Author: [redacted]
Kenneth L. Frack, Jr.

Approved by: [redacted]
Charles W. Therrien, Thesis Advisor

[redacted]
Ralph Hippenstiel, Second Reader

[redacted]
Michael A. Morgan, Chairman,
Department of Electrical and Computer Engineering

ABSTRACT

This thesis examines signal modeling techniques and their application to ambient ocean noise for purposes of noise removal and for generating realistic synthetic noise to add to synthetically generated transient signals. Higher order statistics of the noise are examined to test for Gaussianity. Stochastic approaches to AR, MA, and ARMA modeling are compared to see which technique yields the "best" synthetic noise. Results from the modeling process are used to develop a short-time Wiener filter which can be used to condition a real signal for further processing through effective noise removal.

TABLE OF CONTENTS

LIST OF TABLES

LIST OF FIGURES

I. INTRODUCTION

A. NOISE HINDERS SIGNAL CLASSIFICATION

Ambient ocean noise can significantly reduce the effectiveness of underwater signal classification, both for the human listener and for automatic classifiers such as artificial neural networks. While performance can be improved with adequate training, many transients are rare and occur only in specific locations. This makes it difficult and expensive (if not impossible) to collect a sufficiently large number of examples to perform sufficient training.

Artificial Neural Networks are particularly well suited for pattern classification problems, and their application to underwater transient signal classification continues to be an active area of research. When sufficient training signals are not available however neural networks can classify according to *false clues*. In particular, it is known that in low signal to noise conditions a neural network may classify signals based on characteristics of the noise rather than characteristics of the signal of interest. [1]

Human listeners are similarly plagued by a number of factors which can impair their ability to classify signals in the presence of noise. One of the major problems is that to some extent human listeners hear what they expect to hear. This is especially true when the signal of interest is embedded in noise. As an example, [2] describes an experiment where subjects listened repeatedly to a particular piece of choral music until they knew it very well. The music was then played back to them in the presence of white noise. The signal-to-noise ratio (SNR) was gradually decreased until there was only white noise with no music. All of the subjects *thought* they heard the music playing for a considerable time after the music had been completely turned off. Other physiological effects, such as

masking, *distortion*, and *auditory fatigue* can also impair a human listener's effectiveness as a classifier [3]. Masking, which is when a signal at one frequency seems to hide a signal at another frequency, is extremely important in considering what is heard because it can significantly reduce what one actually hears — the listener could become completely unaware of the fainter frequency components of a complex sound embedded in noise and thus may miss distinguishing characteristics vital to accurate classification [2]. In some cases, problems such as these can be partially overcome with sufficient training, so that the listener learns, through repetition, to discriminate certain signals in the presence of certain noises [3].

B. NOISE HINDERS SIGNAL SYNTHESIS

One method to improve the effectiveness of classification (both for human listeners and artificial neural networks) is to expand the training data. When a sufficient quantity of real data is not available the training data can be expanded by including synthetically generated signals which have all of the significant characteristics of real signals. ARMA modeling techniques have been used both to model transient signals with high precision, and to develop models which are very much like the original, yet distinct. However, the synthesis process typically yields poor results when the signal is corrupted by even a small amount of ambient background noise [4]. The reason for this degradation is that ambient noise, being a broadband process, can only be accurately modeled with high model orders. Thus, in order to accurately model a narrowband process in the presence of wideband noise, excess poles are required [5]. Good models can normally be obtained in the presence of noise if the model order is chosen high enough to account for the broadband nature of the noise. The inclusion of excess poles however can produce undesirable distortions when synthesising new transients from real transient signals [6]. The synthesis is usually bad enough that a human listener can immediately distinguish

between a real signal and a synthetically generated signal. Similarly, the distortions may introduce false clues to artificial neural networks trained with these synthetic signals, and thus cause poor classification performance in a real environment.

C. IMPROVEMENTS THROUGH NOISE MODELING AND FILTERING

Removing noise prior to modeling transients has been shown to greatly improve the ability to generate high quality synthetic training data [6]. Because ambient noise is always present in the ocean environment, once a high quality synthetic signal has been generated, realistic synthetic noise must be added in order to give the synthetic signal convincingly *real* characteristics. Not only must the noise sound real, but a variety of noise sources must be generated so that the classifier learns to classify the signal correctly in the presence of these different sources. The modeling of ocean noise is an extremely important part of the overall process of sonar data modeling and synthesis, since the models are necessary to develop appropriate filters for *removing* noise from the signals of interest before modeling those signals, and the models provide ways to synthesize noise which then can be added to the synthesized signal data in a controlled manner.

This thesis concentrates on two aspects of noise. The first part focuses on the sources of ambient ocean noise and how best to model the noise. Autoregressive (AR), moving-average (MA), and autoregressive moving-average (ARMA) models are compared in terms of simplicity of implementation and quality of reproduction. The comparisons include analysis of the noise spectrums and the model spectrums and subjective listening tests. This modeled noise can be added to synthetically generated transients to produce extremely realistic synthetic transient signals.

The second part of this thesis is directed at developing techniques to remove the noise from digitally recorded signals. Since the signals embedded in the noise are non-stationary,

a non-stationary approach is required. We chose a *short-time* application of the well known Wiener filter because the Wiener filter is an optimal filter for removing noise from a signal. One of the main difficulties in implementing the Wiener filter, however, is that design of this filter requires a knowledge of the signal autocorrelation function and the noise autocorrelation function, and generally assumes that the signal and noise are stationary. Since the respective autocorrelation functions are usually unknown, they must be estimated from the data, with the non-stationarity of the transient signal taken into account. We applied a number of techniques to make the Wiener filter perform satisfactorily in a short-time application with real signals. These techniques include pre-whitening of the signals, filtering short (approximately stationary) signal segments, and overlap averaging of filtered segments.

D. THESIS OUTLINE

The remainder of this thesis is organized as follows. Chapter II discusses the nature of ambient noise and some current models. Results of tests for Gaussianity of the real noise samples examined in this thesis are also presented here. Chapter III describes three modeling techniques, AR, MA, and ARMA modeling, and compares them in the noise modeling application. Chapter IV introduces a noise removal technique which uses a novel implementation of the Wiener filter, and presents results. Chapter V lists conclusions and suggests possibilities for future research.

II. AMBIENT OCEAN NOISE CHARACTERIZATION

Ambient ocean noise studies are typically concerned with being able to *predict* the noise level at certain bandwidths under various climatic and traffic conditions for the purpose of target detection or localization. This thesis analyzes noise from the perspective of trying to *recreate* it in order to 1) develop methods for filtering the noise from real signals and 2) improve the quality of synthetically generated signals by adding synthetically generated noise to these signals. Proper characterization of the recorded noise data is essential for the development of the best statistical models.

The definition of ambient noise varies with the application. Generally, it excludes all noise sources which are identifiable. One of these types of identifiable noise sources is *self noise*. This is any type of noise caused by the recording process, and includes noise from the recording platform such as machinery noise, electronic noise in the amplifier of the receiver, the noise caused by the flow of water over the hydrophone and its support structure, and related sources [7, 8]. Because we do not have control of the recording environment our definition is somewhat more broad; we define ambient noise to include *all* stochastic signals which interfere with the signal of interest, including some noise sources which might be considered identifiable.

There are two reasons for adopting the above definition. First, all noise interferes with the reception of the transient signal of interest, and therefore should be filtered out of the signal in order to obtain the best reproduction of the original transient signal. Secondly, synthetic ambient noise will not adequately represent the noise found with the recorded data if it does not include all sources of noise present in a real environment. For example, if a sonar operator only hears real signals in the presence of flow noise

and machinery noise (two forms of self noise), then these types of noise must also be included in synthetically generated ambient noise to be added to a synthetically generated transient signal so that the synthetic signal will sound exactly like a real signal.

A. SOURCES

The broadband spectrum of ambient ocean noise shows different characteristics at different frequencies, indicating the presence of a variety of noise sources. Since there are several regions of the spectrum where one type of noise source dominates, the spectrum has been typically divided into five somewhat arbitrary frequency bands, each with different prevailing noise sources. The following sections briefly describe some of the primary sources of ambient ocean noise in each region. The descriptions below are summarized from [7, 8], each of which contains a more thorough description of the sources.

1. Ultra-Low Band

This band covers all frequencies less than 1 Hz. It is one of the least significant in terms of underwater sound studies, and is therefore the least studied and understood. The dominant sources in this region include tides, hydrostatic effects of waves, and seismic disturbances. Valid measurements in this frequency range are difficult because of the various sources of self noise caused by the interaction of the hydrophone and its supporting structure with ocean currents, as well as the pyroelectric effect on the hydrophone as tidal currents cause changes in the ocean temperature in the vicinity of the hydrophone.

2. Infrasonic Band

This band, which covers the frequencies from 1 Hz to 20 Hz, is of considerable interest for low frequency passive sonar applications because it contains the blade-rate fundamental frequency of propeller-driven vessels. Thus, one of the major noise sources in

this region is the noise from shipping. In the absence of shipping noise, which dominates all other sources, the noise spectrum in this band depends primarily on wind speed and the level of seismic activity. Self noise caused by the the flow of water over the hydrophone and its supporting structure is also evident in this frequency band. Another source in this region, which is not as significant, is oceanic turbulence in the form of irregular random water currents.

3. Low Sonic Band

This band covers the frequency decade from 20 Hz to 200 Hz, and is dominated by the noise from distant shipping, especially in the frequencies around 100 Hz. It includes sources as far away as 1000 miles. The noise from distant storms competes with the noise from shipping. In the absence of either of these noise sources, the ambient noise level is determined by the local wind speed.

4. High Sonic Band

This band covers the frequencies from 200 Hz to 50 kHz. The noise level in this band depends almost exclusively on the speed of the local wind, especially at frequencies above one kHz. The exact cause of the noise is still uncertain, but it is believed to be caused by a number of interactions of the wind with the water surface. These interactions include the breaking of whitecaps, flow noise of the wind over the water surface, the collapse of air bubbles (cavitation) caused by turbulent wave action, and the wave generating action of the wind.

5. Ultrasonic Band

Thermal noise, which is the noise of molecular bombardment, tends to dominate this band, which covers all frequencies above 50 kHz. This frequency band is not

significant for our purposes since our signals are band limited and were recorded digitally with a sampling frequency much less than 50 kHz.

6. Other Sources

In addition to the noise sources which dominate each of the frequency regions described above there are intermittent sources which can cover more than one frequency band and be persistent enough at times to be considered part of the ambient noise. Biologic noise includes the sounds produced by shellfish, marine mammals, and fish. Non-biologic noise sources include rain, earthquakes, underwater explosions, volcanos, and surf effects. All of these sources are of only limited duration and are therefore not normally considered as part of the ambient background, even though at times they may dominate all other sources. [7]

The ambient noise generated in the arctic has some unique characteristics because of the ice cover, yielding a different noise environment than described above. In addition to the noise sources described above, ambient noise sources in this region include cracking ice, wind over the ice, moving ice masses colliding with each other, and waves impacting ice masses. [7]

B. CHARACTERISTICS

Along with the sources of the ambient noise, there are a number of other considerations which effect the qualities of ambient ocean noise. These characteristics are important to take into account in the development of good noise models.

1. Stationarity

Ambient ocean noise is not stationary because the individual noise sources which contribute to the total noise background are not stationary. For example, biologic activity

is dependent on both the time of day and the season of the year. The noise from shipping similarly varies depending on the time, season, and location. Likewise, noise from the wind and storms is strongly dependent on the local atmospheric conditions. The variability of the ambient noise background over various time intervals is discussed in detail in [7]. Although this variability is real and needs to be taken into account for predicting the noise level at a particular time of the day, we can reasonably assume that the noise is stationary over the short time intervals (several seconds) applicable to the methods described in this thesis since none of the dominant ambient noise sources changes significantly over these short time intervals.

2. Directionality

The strength and spectral shape of the ambient ocean noise also depends on the direction of arrival. With the use of vertical arrays it has been found that shipping noise is highly directional in the horizontal direction, while noise from surface effects, such as wind and rain, are stronger from the vertical direction than from the horizontal direction [7]. Horizontal arrays have similarly been used to show that the noise level in a horizontal plane is determined by such effects as the direction of the wind and swells, as well as the direction of individual ships which contribute to the noise field [7]. In general we do not know the directional characteristics of the recording equipment used to collect the noise samples analyzed in this thesis, so the models we develop do not take the directionality of the noise into account.

3. Depth Dependence

Deep water noise has relatively well-defined levels and is predictable. Shallow water noise however is subject to much wider variations, both in time and location. In deep water the noise level at any given frequency is predominantly from one type of

source, but in shallow water the noise at any frequency is a combination of shipping and industrial noise, wind noise, and noise from biologics. The combination of these three sources is variable and unpredictable, making accurate prediction extremely difficult. [8]

4. Propagation Effects

Sound transmission in the ocean is effected by the water temperature and pressure, with the sound rays bending toward regions of lower temperature and lower pressure. Sound can also reflect off of the sea surface and sea floor. These effects lead to various preferential transmission paths. One of these paths is the *deep sound channel*, in which low frequency sound travels horizontally with little attenuation. A receiver located in the deep sound channel will detect more noise than a receiver located below the channel. Similarly, noise from the sea surface can be trapped in the *surface duct* and travel nearly horizontally to distant locations. When the conditions are right, both the deep sound channel and the surface duct are likely to be noisy environments. The propagation of sound is also dependent on frequency, with high frequencies being attenuated much more than low frequencies. This causes the ocean to behave as a low pass filter. [7]

C. STATISTICS

The most important aspect of the noise from the standpoint of modeling and filtering is its statistical characteristics. Ambient ocean noise, which is comprised of many individual sources, is typically assumed to have a Gaussian distribution over short periods of time [7]. This assumption is based on the *Central Limit Theorem*, which states that the probability distribution of a sum of a very large number of random variables *approaches* a Gaussian distribution [9]. This assumption however is not valid in every case, particularly in the presence of dominant non-Gaussian noise sources (such as impulsive noise) [10, 11]. Testing the noise to see if truly it has a Gaussian amplitude distribution

is important in determining the most suitable techniques for modeling and filtering the noise. If the noise has a Gaussian distribution, then linear methods will yield optimal results [12]. For processes with non-Gaussian distributions, non-linear techniques are generally required in order to obtain optimal results.

We tested both real and synthetically generated noise sources using a variety of statistical methods. The synthetic noise sequences were generated using *Matlab* [13], and were included to provide a "benchmark" with which to compare the results from the real data. The real data used was collected from a variety of underwater transient sources. In all cases the data sequences consisted only of background noise extracted before onset of the actual transient signal. The noise sequence labeled *orca* is from a recorded biologic (a killer whale). The *tk-10a* noise is from ocean data distributed by DARPA to contractors as part of an early test of classification algorithms. The noise sequence *bio-2385* is part of the NUSC *TAP06* data. Finally, the sequences *wx01*, *qx03*, and *fx09* are ambient noise from sounds recorded during range tests.

1. χ^2 Test for Gaussianity

It would be extremely difficult to absolutely prove that a sequence has a Gaussian distribution because no matter how much evidence is collected there always exists the possibility that it does not. We can relatively easily prove that a sequence does *not* have a Gaussian distribution however. This is how the χ^2 test is used as a means of testing for Gaussianity. A null hypothesis (H_0) that the sequence has a Gaussian amplitude distribution is formulated. The alternate, and mutually exclusive, hypothesis (H_1) is that the sequence does *not* have a Gaussian amplitude distribution. We accept H_0 as being true only if there is insufficient evidence to reject H_1. The decision to accept or reject the null hypothesis at a certain *level of significance* is based on comparing the computed χ^2 *test statistic*, a weighted summation of the difference between the observed

and expected probability distributions of the data, with a pre-determined *critical value.* The null hypothesis is accepted (at the desired level of significance) if the test statistic is less than the critical value. [14, 15]

To perform the test the data are first categorized into r amplitude cells. The number and size of the cells is flexible and typically depends on the application, but in general one should choose as many cells as possible in order to increase the number of degrees of freedom, with the condition that the expected number of occurrences in each cell should be at least five [16, 14]. Since the data will be distributed among the r cells according to the probability distribution function of the data, the number of degrees of freedom v is $r - 1$ (the number of occurrences in cell r is determined by the number of occurrences in the previous $r - 1$ cells). If the expected cell probabilities depend on unknown parameters which must be estimated from the data, then an additional degree of freedom must be subtracted for each unknown parameter [15]. Since a Gaussian process is completely characterized by its mean and variance, these are the only parameters which must be estimated from the data to test for a Gaussian fit. Thus, for all of our sequences the number of degrees of freedom is $v = r - 1 - 2 = r - 3$.

The test statistic W is computed by forming a weighted sum of the squared differences between the actual number of occurrences in each cell and the number of occurrences in each cell which would be expected of a Gaussian sequence. This weighted sum is given by

$$W = \sum_{i=1}^{r} \frac{(N_i - e_i)^2}{e_i} \tag{2.1}$$

where r is the number of amplitude cells, N_i is the actual number of occurrences in cell i, and e_i is the observed number of occurrences in cell i. If the data sequence represents a multinomial experiment of N_s independent trials, then as N_s approaches infinity the distribution W approaches a χ^2 distribution with v degrees of freedom. [15]

In order to obtain a meaningful value for the test statistic we used, when possible, $N_s = 20000$ points of the noise sequence. This usually allowed us to form as many as 25 equally spaced amplitude cells and still maintain $e_i \geq 5$ for all but one or two cells at each tail. The cells at either tail with $e_i < 5$ were combined so that all cells had $e_i \geq 5$ [15]. We chose a level of significance of 0.05, which represents the risk involved in wrongly deciding to reject the null hypothesis (the probability that the null hypothesis was incorrectly rejected).

Table 2.1 shows the results of the χ^2 test for a number of different synthetically generated noise sequences. In each case the number of degrees of freedom v was chosen

Noise Source	N_s	r	v	W	$\chi^2_{0.05,v}$	Gaussian?
Gaussian	20000	23	20	18.82	31.41	yes
uniform	20000	25	22	4874.0	33.92	no
12 uniforms	20000	23	20	12.70	31.41	yes
Laplacian	20000	15	12	3619.4	21.03	no
exponential	20000	11	8	16629	15.51	no
Bernoulli-Gaussian	20000	21	18	338.7	28.87	no

TABLE 2.1: RESULTS OF THE χ^2 TEST FOR GAUSSIANITY USING SYNTHETICALLY GENERATED NOISE SEQUENCES.

as three less than r, the number of cells with $e_i \geq 5$. The Gaussian and uniform white noise sequences were generated using the intrinsic *Matlab* functions "randn" and "rand," respectively. The Laplacian, exponential, and Bernoulli-Gaussian (with event probability 0.95) noise sources were generated using the "rpiid" function from the *Matlab* "Hi-Spec" toolbox [17]. Notice that only the Gaussian sequence and the sequence formed by summing twelve independent realizations of 20000 points of uniform noise passed the χ^2 test for Gaussianity at the 0.05 significance level.

The test was then performed on the real noise sequences described earlier. The results are listed in Table 2.2. With the exception of the sequence *orca* all of the recorded

noise sequences passed the test well within the five percent significance level, providing strong evidence that these noise sequences have distributions which do not significantly depart from Gaussianity. The sequence *orca* is apparently *not* Gaussian, however its deviation from Gaussianity does not appear to be strong.

Noise Source	N_s	r	v	W	$\chi^2_{0.05,v}$	Gaussian?
orca	12000	21	18	31.56	28.87	no
tk-10a	20000	23	20	17.12	31.41	yes
bio-2385	20000	21	18	12.99	28.87	yes
wx01	20000	21	18	12.94	28.87	yes
qx03	20000	23	20	11.13	31.41	yes
fx09	20000	21	18	10.20	28.87	yes

TABLE 2.2: RESULTS OF THE χ^2 TEST FOR GAUSSIANITY USING RECORDED OCEAN NOISE.

The χ^2 test has some important limitations. One of these limitations is that the distribution of the discrepancies between the observed and expected frequencies is not taken into account, even though this distribution may influence how well the data appear to fit the theoretical curve. In other words, we would expect that the difference $N_i - e_i$ should alternate randomly between positive and negative values. If however, the differences are positive for all cells higher than the mean and negative for all cells lower than the mean, then the data would be less likely to have a Gaussian distribution, even though the χ^2 test statistic gives a satisfactory result. [18]

Another important limitation of the χ^2 test is that it considers only the *marginal* first and second order statistics (the mean and the variance) of the sequence, which is insufficient to prove *joint* Gaussianity [19]. Other more powerful tests such as those discused in the next section are sensitive to joint properties of the data.

2. Gaussianity Tests Based on Higher-Order Statistics

Tests based on higher order statistics (HOS) can yield additional insight since they are not necessarily subject to the same limitations as the χ^2 test. Classical tests are based on simple calculations of the marginal third and fourth order *moments*, while modern tests are based on the third and fourth order *cumulants*. These modern tests yield more information, but typically require significantly more calculations than classical tests, and have thus only lately gained increased attention because of the recent improvements in the computational capabilities of modern computers.

a. Classical Tests

Two classical tests are the measures of the coefficient of *skewness* and the coefficient of *kurtosis* of a random sequence. The coefficient of skewness is a measure of the symmetry of the density function about the mean. A Gaussian density function, and all other symmetric density functions, have zero skewness. For this reason the coefficient of skewness by itself is not a valid test for Gaussianity of a data sequence. Its usefulness is in showing that a density function is *not* Gaussian since non-zero skewness is incompatible with Gaussianity. The coefficient of kurtosis, which is a measure of peakedness of the density function, can provide additional insight. Its value is zero for a Gaussian density function. A density function with a sharper peak (such as the Laplacian density) has a positive coefficient of kurtosis and is called *leptokurtic*, while a density function with a negative coefficient of kurtosis has a flatter peak and is called *platykurtic*. [15]

The coefficients of skewness and kurtosis rely on the calculations of the marginal third and fourth order central moments about the mean of the sequence (Since only the marginal statistics are considered, as with like the χ^2 test, these tests are

insufficient to prove joint Gaussianity.) The k^{th} central moment about the mean of a random variable X is defined as

$$\mu_k = \mathcal{E}[(X - m_X)^k] \tag{2.2}$$

where m_X is the mean of the random variable and $\mathcal{E}[\cdot]$ represents the expectation operation. These statistical parameters are generally unknown, so they must be estimated from the data. The sample mean is estimated by

$$\hat{m}_X = \frac{1}{N_s} \sum_{n=0}^{N_s-1} x(n) \tag{2.3}$$

while the sample variance of the data, which is the second central moment about the mean, is estimated by

$$\hat{\sigma}_X^2 = \frac{1}{N_s} \sum_{n=0}^{N_s-1} [x(n) - \hat{m}_X]^2 \tag{2.4}$$

from which the sample standard deviation $\hat{\sigma}_X$ can be obtained. Using (2.3), the sample third and fourth central moments about the mean are then estimated by

$$\hat{\mu}_3 = \frac{1}{N_s} \sum_{n=0}^{N_s-1} [x(n) - \hat{m}_X]^3 \tag{2.5}$$

$$\hat{\mu}_4 = \frac{1}{N_s} \sum_{n=0}^{N_s-1} [x(n) - \hat{m}_X]^4 \tag{2.6}$$

Finally, using (2.3), (2.4), (2.5), and (2.6), the coefficient of skewness α_3 and coefficient of kurtosis α_4 are estimated by [15]

$$\hat{\alpha}_3 = \frac{\hat{\mu}_3}{\hat{\sigma}_X^3} \tag{2.7}$$

$$\hat{\alpha}_4 = \frac{\hat{\mu}_4}{\hat{\sigma}_X^4} - 3 \tag{2.8}$$

The test yields *qualitative* rather than *quantitative* results since no test statistic is computed as with the χ^2 test. A sequence can be considered non-Gaussian if either quantity is not close to zero. Table 2.3 lists the results of these tests for the same test

Noise Source	n	skewness ($\hat{\alpha}_3$)	kurtosis ($\hat{\alpha}_4$)
Gaussian	20000	-0.0024	0.0122
uniform	20000	0.0024	1.8002
12 uniforms	20000	-0.0020	-0.0149
Laplacian	20000	0.0118	2.9975
exponential	20000	1.9386	5.3594
Bernoulli-Gaussian	20000	0.0155	0.1912

TABLE 2.3: RESULTS OF THE TESTS OF SKEWNESS AND KURTOSIS USING SYNTHETICALLY GENERATED NOISE SEQUENCES.

noise sequences as those listed in Table 2.1. All of the sequences except the exponential sequence have small coefficients of skewness, indicating that only the exponential sequence fails the test for Gaussianity based on symmetry properties. The other non-Gaussian sequences (uniform, Laplacian, and Bernoulli-Gaussian) passed the test of zero skewness but failed the test of Gaussianity based on their respective coefficients of kurtosis, illustrating the importance of performing both tests. Only the Gaussian and the twelve uniform sequences added together passed the test for Gaussianity based on both the coefficient of skewness and the coefficient of kurtosis.

Table 2.4 lists the results for the real noise sequences. All of these sequences except *orca* have coefficients of skewness and kurtosis close to zero, giving strong evidence that the sequences may be Gaussian. The sequence *orca* is possibly non-Gaussian since its coefficient of kurtosis is relatively large. This sequence is the only one that also did not pass the χ^2 test at the 0.05 significance level.

b. Tests Based on Higher Order Cumulants

Characterization of random processes using higher-order moments is a field which has recently been given much attention. *Cumulants*, which are related to moments, can be used for characterizing random processes, and are particularly useful as a measure

Noise Source	n	skewness ($\hat{\alpha}_3$)	kurtosis ($\hat{\alpha}_4$)
orca	12000	0.0055	0.1017
tk-10a	20000	0.0042	-0.0504
bio-2385	20000	0.0044	-0.0274
wx01	20000	-0.0028	-0.0333
qx03	20000	-0.0007	-0.0069
fx09	20000	-0.0111	0.0507

TABLE 2.4: RESULTS OF THE TESTS OF SKEWNESS AND KURTOSIS USING RECORDED OCEAN NOISE.

of departure from Gaussianity since all cumulants of order higher than two are identically zero for a Gaussian random process. If x is a real zero-mean random process the first four cumulants are

$$C_x^{(1)} = \mathcal{E}[x(n)] = m_x = 0 \tag{2.9}$$

$$C_x^{(2)}(l_1) = \mathcal{E}[x(n)x(n+l_1)] = R_x(l_1) \tag{2.10}$$

$$C_x^{(3)}(l_1, l_2) = \mathcal{E}[x(n)x(n+l_1)x(n+l_2)] \tag{2.11}$$

$$\begin{aligned} C_x^{(4)}(l_1, l_2, l_3) = {} & \mathcal{E}[x(n)x(n+l_1)x(n+l_2)x(n+l_3)] - C_x^{(2)}(l_1)C_x^{(2)}(l_3 - l_2) \\ & - C_x^{(2)}(l_2)C_x^{(2)}(l_3 - l_1) - C_x^{(2)}(l_3)C_x^{(2)}(l_2 - l_1) \end{aligned} \tag{2.12}$$

where the arguments l_1,l_2, and l_3 are referred to as "lag values." Note that if the sequence x has unit variance then for $l_1, l_2, l_3 = 0$ (2.11) and (2.12) reduce to (2.7) and (2.8). respectfully. Since the third order cumulant is related to the skewness of the density function, tests based only on the third order cumulant are insufficient to completely determine Gaussianity for the same reason that the coefficient of skewness is an inadequate test when performed by itself. The fourth order cumulant, like the coefficient of kurtosis, should also be considered when testing for Gaussianity. Cumulants of order higher than four are not typically used since they are difficult to compute reliably and thus have little practical application. [12]

The *power spectrum* of a sequence can be obtained as the one-dimensional Fourier transform of the second order cumulant (which is identical to the covariance for a zero mean process). *Higher-order spectra*, or *polyspectra*, can be similarly obtained as multidimensional Fourier transforms of higher-order cumulants. In particular, the two-dimensional Fourier transform of the third-order cumulant is called the *bispectrum*, and is expressed as

$$B_x(\omega_1, \omega_2) = \sum_{l_1=-\infty}^{\infty} \sum_{l_2=-\infty}^{\infty} C_x^{(3)}(l_1, l_2) e^{-j(\omega_1 l_1 + \omega_2 l_2)} \tag{2.13}$$

For a real random process the bispectrum has twelve regions of symmetry, so the bispectrum needs to be computed only over the triangular non-redundant region [20]

$$\Omega = \{0 \leq \omega_1 \leq \pi,\ \omega_2 \leq \omega_1,\ 2\omega_1 + \omega_2 \leq 2\pi\} \tag{2.14}$$

The rest of the bispectral plane is related to points in this region through symmetry properties and thus contains no new information. [12]

The normalized bispectrum (or *bicoherence*) is

$$B_x^{(n)}(\omega_1, \omega_2) = \frac{B_x(\omega_1, \omega_2)}{\sqrt{S_x(\omega_1) S_x(\omega_2) S_x(\omega_1 + \omega_2)}} \tag{2.15}$$

where $S_x(\omega_i)$ is the power spectrum of the sequence x at frequency ω_i. Using (2.15) the *average* skewness of the sequence is

$$\bar{\alpha}_3 = \frac{1}{2\pi} \iint B_x^{(n)}(\omega_1, \omega_2)\, d\omega_1\, d\omega_2 \tag{2.16}$$

where the integration is performed over the non-redundant region defined by (2.14). This relationship is the basis for using the estimated bicoherence of the sequence to compute a test statistic which gives the probability of falsely rejecting the hypothesis of zero skewness. [20]

The *Matlab* function "GLSTAT" from the "Hi-Spec" toolbox was used to perform this test. "GLSTAT" first estimates the bispectrum using a direct Fourier

transform approach, from which the bicoherence is estimated. The test statistic, which is the mean bicoherence power, is computed as

$$S = \sum |\hat{B}_x^{(n)}(\omega_1, \omega_2)|^2 \tag{2.17}$$

where the summation is performed over the non-redundant region defined by (2.14). The test statistic S has a χ^2 distribution with the number of degrees of freedom determined by the length of the discrete Fourier transform (DFT) length and and the resolution parameter. This test is described in detail in [20] and [17].

Table 2.5 lists the results from testing the same noise sequences listed in Table 2.1 and Table 2.3. N_s is the number of points in the data sequence, S is the test

Noise Source	N_s	S	P_{FA}	Symmetric?
Gaussian	20000	0.7444	1.0000	yes
uniform	20000	0.4885	1.0000	yes
12 uniforms	20000	0.5393	1.0000	yes
Laplacian	20000	0.8936	1.0000	yes
exponential	20000	167.80	0.0000	no
Bernoulli-Gaussian	20000	0.7281	1.0000	yes

TABLE 2.5: RESULTS OF HINNICH'S TEST FOR GAUSSIANITY USING SYNTHETICALLY GENERATED NOISE SEQUENCES.

statistic, and P_{FA} is the probability of incorrectly accepting the non-zero skewness hypothesis. The DFT length for all sequences was 256 points and the resolution parameter was chosen as 0.51 (the default value used by the "GLSTAT" function), which resulted in 48 degrees of freedom for all data sequences. If the P_{FA} is high there is strong evidence that the non-zero skewness hypothesis can be rejected in favor of the zero skewness hypothesis. If the P_{FA} is lower than about 0.05 the probability is high that the data have non-zero skewness, and are therefore non-Gaussian. All of the noise sequences, with the exception of the exponential sequence, had high values of P_{FA}, indicating that the zero skewness hypothesis can not easily be rejected.

Table 2.6 lists the results from testing the same noise sequences listed in Table 2.2 and Table 2.4. All of the real noise sequences passed the test. We noticed

Noise Source	N_s	S	P_{FA}	Symmetric?
orca	12000	21.750	0.9996	yes
tk-10a	20000	1.0470	1.0000	yes
bio-2385	20000	52.970	0.2882	yes
wx01	20000	0.5171	1.0000	yes
qx03	20000	0.5502	1.0000	yes
fx09	20000	0.9484	1.0000	yes

TABLE 2.6: RESULTS OF HINNICH'S TEST FOR GAUSSIANITY USING RECORDED OCEAN NOISE.

that the DFT length can significantly affect the values of both the test statistic S and the P_{FA} for a correlated noise sequence, indicating the importance of not rejecting the zero-skewness hypothesis based on performing the test using only one DFT length. For example, we found that a colored Gaussian noise sequence failed the above test using a DFT length of 256, but passed the test using a DFT length of 255 or 257. Similarly, the P_{FA} for sequence *bio-2385* was only 0.2882 with a DFT length of 256 but was 0.9986 with a DFT length of 257. Although we do not have a detailed explanation, we assume that the variation is due to some anomaly (such as periodicity) introduced into the data at or near a specific DFT length that does not otherwise appear.

Because of the computational complexity involved with estimating the fourth-order cumulant, efficient quantitative statistical tests based on the fourth order cumulant have not yet been developed. Therefore a qualitative test was performed in the same way that the qualitative tests were performed using the coefficients of skewness and kurtosis. Since the fourth order cumulant is cumbersome to estimate for all lag values one can obtain a "sample" of it by estimating its value on a one-dimensional *slice* (i.e., a line through the space of lag values). Although any one-dimensional slice can be used, we

chose the *diagonal* slice, which is equivalent to setting $l_1 = l_2 = l_3$ in (2.12). The maximum value of this one-dimensional slice is compared with the theoretical value of zero. If this maximum value significantly deviates from zero then there is a strong possibility that the sequence is not Gaussian.

The *Matlab* function "CUMEST" from the "Hi-Spec" toolbox was used to estimate the diagonal slice of the fourth order cumulant, $\hat{C}_x^{(4,d)}$, using the "overlapped-segment method" described in [17]. The biased estimate was computed using a segment length of 1000 points with 50 percent overlap, and lag values ranging from $l = -100$ to $l = +100$. The results are listed in Tables 2.7 and 2.8.

Noise Source	N_s	$\max(\hat{C}_x^{(4,d)})$
Gaussian	20000	0.0534
Uniform	20000	-1.2011
12 uniforms	20000	-0.0491
Laplacian	20000	3.1137
exponential	20000	6.2762
Bernoulli-Gaussian	20000	0.1939

TABLE 2.7: RESULTS OF THE TEST FOR GAUSSIANITY USING THE DIAGONAL SLICE OF THE FOURTH ORDER CUMULANT OF SYNTHETICALLY GENERATED NOISE SEQUENCES.

The results listed in Table 2.7 are similar to the results from testing for the coefficient of kurtosis listed in Table 2.3. Note that only the Gaussian noise sequence and the sequence formed by summing 12 independent uniform sequences yielded low values for the maximum value of $\hat{C}_x^{(4,d)}$. The other synthetic noise sequences had high values for $\hat{C}_x^{(4,d)}$, indicating that they have a low probability of being Gaussian.

The results listed in Table 2.8 are likewise similar to the results from testing for the coefficient of kurtosis listed in Table 2.4. All of the real sequences, with the exception of *orca*, yielded small values of $\hat{C}_x^{(4,d)}$, indicating that these sequences do not

Noise Source	N_s	$\max(\hat{C}_x^{(4,d)})$
orca	20000	0.1242
tk-10a	20000	-0.0603
bio-2385	20000	-0.0705
wx01	20000	0.0543
qx03	20000	0.0607
fx09	20000	0.0407

TABLE 2.8: RESULTS OF THE TEST FOR GAUSSIANITY USING THE DIAGONAL SLICE OF THE FOURTH ORDER CUMULANT OF RECORDED OCEAN NOISE.

significantly deviate from Gaussianity. The relatively large maximum value of $\hat{C}_x^{(4,d)}$ for *orca* indicates that this sequence is possibly non-Gaussian. This departure from Gaussianity however is not strong since the maximum value of $\hat{C}_x^{(4,d)}$ for *orca* is not nearly as large as that obtained for the known non-Gaussian noise sequences.

3. Statistical Conclusion

The results of the statistical tests indicate that all of the recorded noise sequences we considered in this thesis can reasonably be assumed to have a Gaussian distribution. Most of the noise sequences responded to the test with strong evidence of Gaussianity. Only the *orca* noise sequence gave evidence of non-Gaussianity and the evidence in most tests was not strong. These results imply that linear Gaussian techniques are appropriate vehicles to obtain models and filters for these noise sequences. This is fortunate, since very few real processes if non-Gaussian are linear [21] and methods for modeling of non-linear and non-Gaussian random processes are only in the early stages of development.

III. MODELING

The process of signal modeling involves designing a filter to produce a sequence with characteristics which are identical to a desired random process. In our case the desired random process is ambient ocean noise. Because the recorded ocean noise tends to have a Gaussian distribution, only the second-order statistics of the original sequence need to be matched (a Gaussian process is completely defined by its second-order statistics). Since a linear transformation of a Gaussian random process preserves its Gaussian nature, an appropriate signal model is a *linear* model driven by Gaussian white noise. Additionally, since the recorded noise also tends to be stationary over the time intervals of interest, a time-invariant model can be used. Finally, since we desire stable models with stable inverses for the application described in Chapter IV, the models we shall focus on will be minimum phase linear models.

A. TYPES OF LINEAR MODELS

Three basic linear time-invariant models are considered: the *autoregressive* (AR), the *moving average* (MA), and the *autoregressive moving average* (ARMA) models. These models are illustrated in Figure 3.1, where $w(n)$ is a Gaussian white noise sequence of unit variance, $x(n)$ is the modeled sequence, and $A(z)$ and $B(z)$ are the polynomials in the denominator and numerator, respectively, of the filter transfer function defined by

$$A(z) = a_0 + a_1 z^{-1} + a_2 z^{-2} + \cdots + a_P z^{-P} \tag{3.1}$$

and

$$B(z) = b_0 + b_1 z^{-1} + b_2 z^{-2} + \cdots + b_Q z^{-Q} \tag{3.2}$$

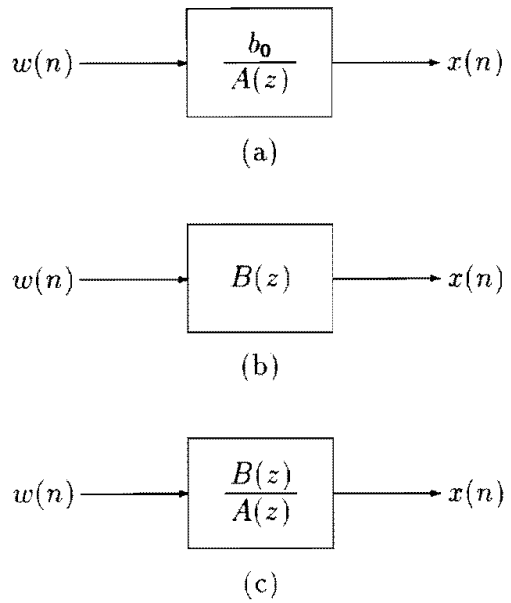

Figure 3.1: Types of Linear Models. (a) AR. (b) MA. (c) ARMA

All three models can be described in the time domain by the difference equation for the general ARMA model,

$$x(n) + a_1 x(n-1) + \cdots + a_P x(n-P) = b_0 w(n) + b_1 w(n-1) + \cdots + b_Q w(n-Q) \quad (3.3)$$

The AR model can be obtained from (3.3) by setting $P \neq 0$ and $Q = 0$; the MA model can be obtained by setting $P = 0$ and $Q \neq 0$. [12]

Because the AR model can have *poles* near the unit circle, the AR model is best for representing sequences with *peaks* in the power spectrum. Correspondingly, since the MA model can be designed with *zeros* near the unit circle, the MA model is best for representing sequences with *nulls* in the power spectrum. The ARMA model works well for sequences with both peaks and nulls in the power spectrum, as well as other general spectra without pronounced peaks and nulls. The models are somewhat interchangeable in that an AR model can be used to estimate an ARMA or MA process if the model order is chosen sufficiently high and a MA model can be used to estimate an AR or ARMA

process with a high enough model order. The best results are obtained however when the model exactly matches the process which generated the sequence. [12]

1. The AR Model

The simplest model to solve is the AR or *all-pole* model because its solution depends entirely on a system of linear equations. We chose to use Burg's method [12] to find the a_i's of (3.1) because it ensures a *minimum phase* solution (all roots of $A(z)$ inside the unit circle) and so guarantees that both the model and its inverse will be stable.

Since Burg's method is based on a least squares procedure, better results are obtained if the noise sequences to be modeled are very long. Using 10,000 to 20,000 points gives the best results without taking too much time to compute. Using more than 20,000 points serves only to increase the computation time without providing better results. Using less than a few thousand points does not seem to capture enough of the noise characteristics to obtain the best models.

2. The MA Model

The MA, or *all-zero*, model, even though it seems to have the simplest form, is in general difficult to solve because its solution depends on a system of nonlinear equations. If the sequence to be modeled was generated by an MA process, then the transfer function polynomial can be obtained by *spectral factorization* of the *spectral density function* of the original process. The spectral density function $S_x(z)$ is found by taking the z-transform of the autocorrelation function of the random process. Since for a white noise input $S_x(z)$ is of the form

$$S_x(z) = B(z)B^*(1/z^*) \tag{3.4}$$

$B(z)$ can be solved for by finding the roots of $S_x(z)$. Multiple solutions are generally possible because the roots of $S_x(z)$ occur in complex reciprocal locations, giving rise to

minimum phase, maximum phase, and possibly mixed phase solutions for $B(z)$. If the signal to be modeled is deterministic or non-Gaussian it is important to choose the roots with the correct phase in order to obtain an accurate model. If the signal to be modeled is a Gaussian random process, then the maximum phase, mixed phase, or minimum phase solutions are all equally valid since each of these models yields identical second order statistics. However since subsequent processing requires the inverse of the filter, we chose the minimum phase solution of $B(z)$ by selecting the roots of $S_{\boldsymbol{x}}(z)$ which lie inside the unit circle. [12]

The MA model turned out to be ineffective for our purpose for two reasons. First, models of low order generally do not yield well modeled noise. Higher order models can improve the quality of the modeled noise, but these higher model orders usually have zeros of $B(z)$ close to or on the unit circle, which causes stability problems for the inverse model. Secondly, the spectral factorization is subject to errors. The factorization algorithm does not always yield the same number of minimum and maximum phase roots, and poles on the unit circle rarely occur in even multiplicities. These errors may be attributed to roundoff error in factoring $S_{\boldsymbol{x}}(z)$ and the error associated with estimating the correlation function of the original noise sequence.

3. The ARMA Model

The ARMA, or *pole-zero*, model is the most flexible of the models and typically requires the fewest number of model parameters. *Optimal* methods for estimating the ARMA model parameters involve solving for the AR and MA parameters simultaneously. Unfortunately, optimal methods (usually iterative and based on maximum likelihood or related concepts) are not well developed because they require the solution of a system of highly nonlinear equations, and may not converge to a correct solution. The preferable methods are *suboptimal*, and usually involve solving for the AR and MA parameters

separately. The advantage to these techniques is the significantly reduced computational complexity. If the original random process was truly generated by an ARMA process the model can be obtained by finding the AR parameters first and then filtering the original sequence by the filter formed from the AR parameters, yielding a *residual* sequence which is a pure MA process. The MA parameters can then be found by spectral factorization of the residual sequence. [22, 23]

The main advantage of ARMA modeling for deterministic signals is that it generally yields the most *parsimonious* representation of the original sequence [12]. This is of tremendous usefulness in applications where data compression or simplicity are important. Consequently, ARMA models are favored for modeling transient signals. (For example, a 2000 point transient signal could be modeled by segmenting the data into, say, forty fifty-point segments, and then modeling each segment with perhaps a $(P, Q) = (6, 5)$ ARMA model. The modeled transient then has only 440 parameters instead of the original 2000.) For noise modeling, however, a parsimonious representation is not necessarily advantageous because any sequence of stationary noise, regardless of length, requires only one model, and therefore only one set of calculations. (One is not normally interested in purposefully transmitting compressed noise.)

For modeling noise the ARMA model does not give better results than the AR model because it suffers from the same pitfalls as the MA model: spectral factorization errors and inverse filters with poor stability characteristics. Additionally, any reduction in parameters in the ARMA over the AR model for noise is usually offset by the increased computational complexity of finding the ARMA model parameters.

B. MODEL ORDER SELECTION

Choosing the correct model order for stochastic data is not a *trivial problem*. We analyzed four methods for determining the best model order for our data. Theoretically,

if the data can be described by a finite order AR model and if the model order is chosen correctly, then the theoretical prediction error variance will remain constant for all model orders higher than the theoretical model order. Real data is seldom generated by an exact AR process, so it may be difficult to find the model order at which the prediction error variance becomes constant. This section examines a number of methods to approximate the best model order.

1. Theoretical Criteria

The four most common methods for chosing the model order seek to minimize a quantity related to the prediction error variance $\sigma^2_{\epsilon_P}$ and the number of data points N_s. These quantities, which each have a distinct minimum at the optimal model order, are Akaike's information-theoretic criteria (AIC), Parzen's criterion autoregressive transfer (CAT), Akaike's final prediction error (FPE), and Schwartz and Rissanen's minimum description length (MDL). The formulas for these quantities are

$$\mathrm{AIC}(P) = N_s \ln \sigma^2_{\epsilon_P} + 2P \tag{3.5}$$

$$\mathrm{CAT}(P) = \left(\frac{1}{N_s} \sum_{p=1}^{P} \frac{N_s - p}{N_s \sigma^2_{\epsilon_p}} \right) - \frac{N_s - P}{N_s \sigma^2_{\epsilon_P}} \tag{3.6}$$

$$\mathrm{FPE}(P) = \sigma^2_{\epsilon_P} \left(\frac{N_s + P + 1}{N_s - P - 1} \right) \tag{3.7}$$

$$\mathrm{MDL}(P) = N_s \ln \sigma^2_{\epsilon_P} + P \ln N_s \tag{3.8}$$

Figure 3.2 demonstrates the use of one of these criteria, the AIC, which does indeed have a minimum at $P = 17$. Unfortunately, since these quantities work well only if the data are generated by an AR process, their use can be severely limited for real data. [12]

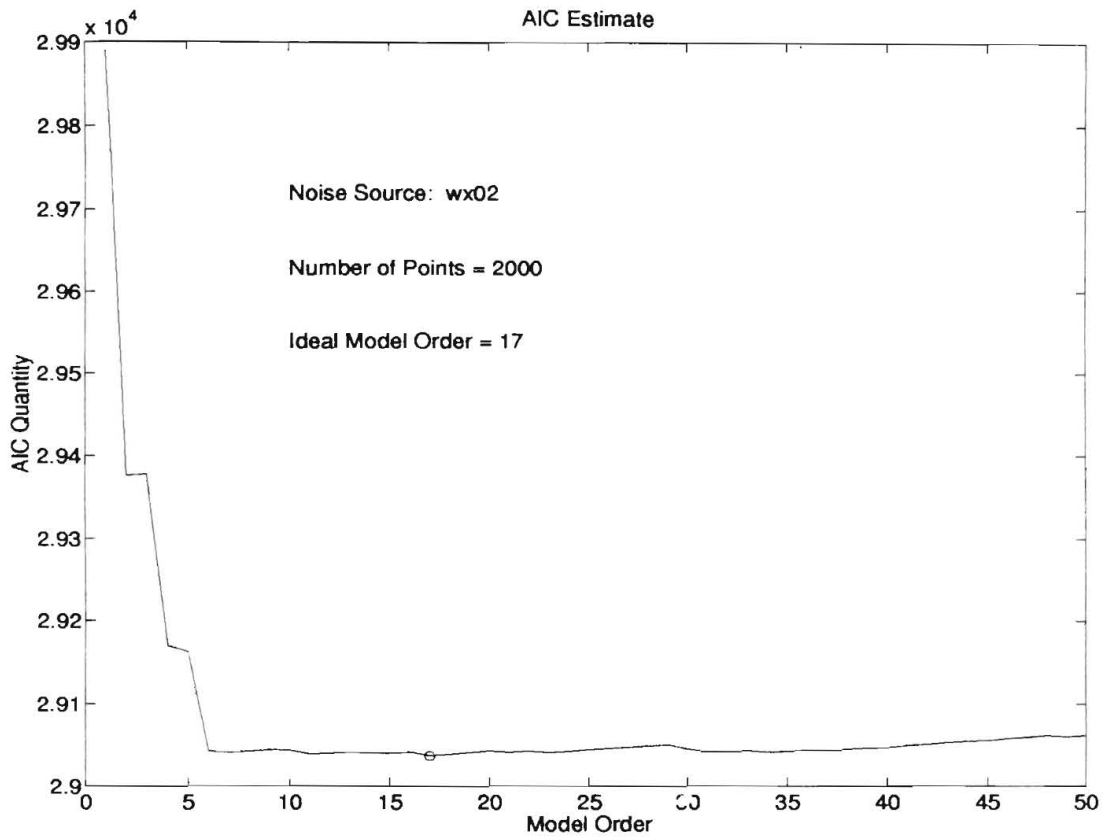

Figure 3.2: Example of Model Order Selection Based on the AIC Criteria for Sequence *wx02* Using 2000 Points of Noise Data .

One major drawback of these criteria for modeling stochastic data is their dependence on the data length. Long sequences of data (on the order of 10,000 points) typically indicate very high filter orders, while short data sequences (on the order of 1000 points) typically yield much lower filter orders. For example, when the data sequence *wx02* was tested using 2000 points of noise, a 17^{th} order model was indicated, while using 20,000 points of noise indicated that a 98^{th} order model should be used. The dilemma is that the accuracy of least-squares techniques, such as Burg's method, improve with increasing data length, thereby yielding better model parameters. The theoretical model

orders indicated by the above methods can indicate erroneously high model orders however, and are therefore only of limited usefulness in modeling stochastic data which are not generated by a truly AR process.

2. Computation of Prediction Error

In this analysis the prediction error for linear predictive filtering was computed and tested. For a well chosen model order the output of the prediction error filter pictured in Figure 3.3 will be Gaussian white noise of unit variance. The filter transfer function

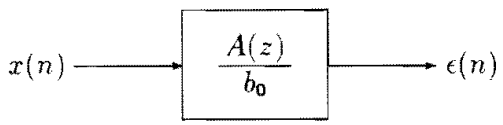

Figure 3.3: Prediction Error Filter.

is given by (3.1) where the a_i parameters are the same as those in (3.3). For each model order selected, the original data was filtered with the prediction error filter and the spectrum of the resulting error signal was analyzed. The model order was chosen as the lowest order which gave a reasonably flat spectrum for the error signal. Figure 3.4 shows an example of using the spectrum of the PEF output. In this example an 11^{th} order AR model was used to model 20,000 points of noise from the sequence *wx02*. Notice that the variation for the PEF output spectrum is slightly greater than the variation of the spectrum for the white noise. The variance could be reduced by a slightly higher order model but other tests described below give some rationale for retaining the 11^{th} order AR model.

3. Spectral Density Comparison

In this test, the AR parameters for the noise are obtained using Burg's method as before. The model in Figure (3.1)(a) is then driven with Gaussian white noise of

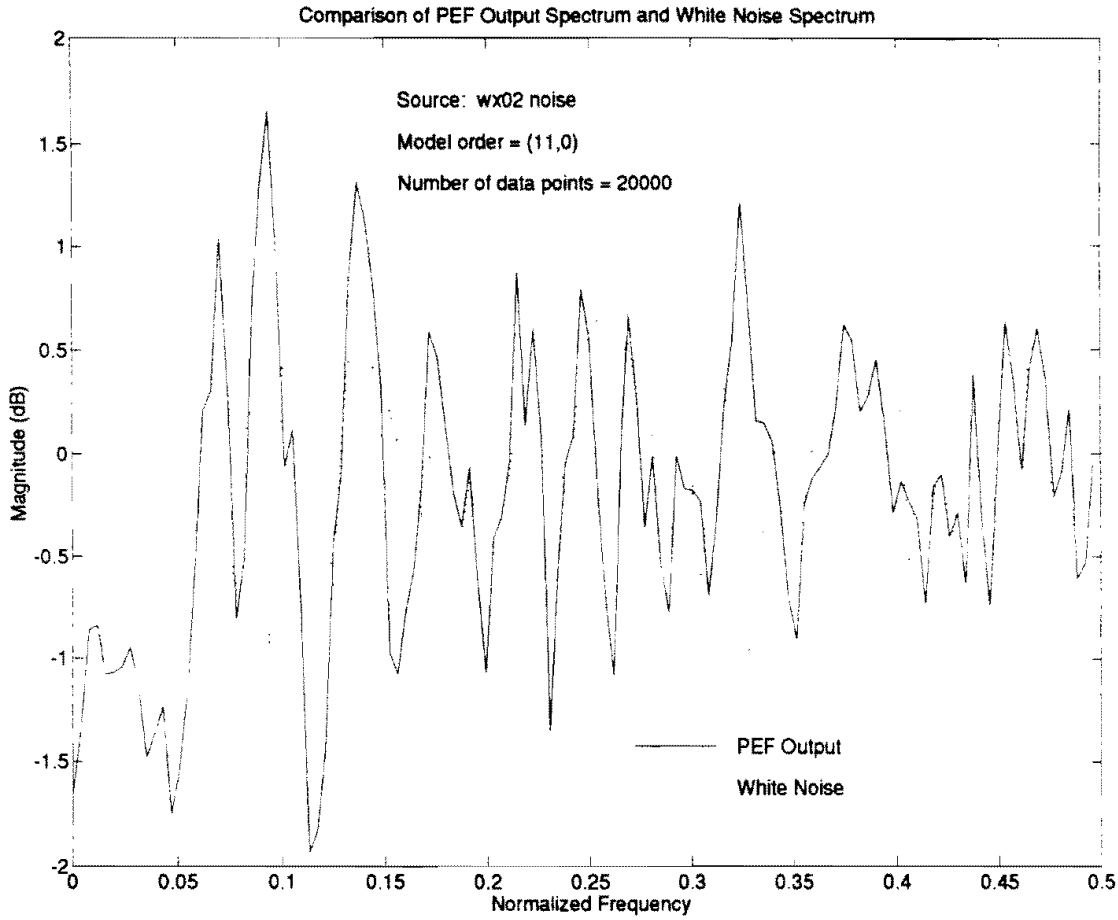

Figure 3.4: Example of Model Order Selection Based on the Flatness of the Prediction Error Filter Output Spectrum for Sequence *wx02* Using 20,000 Points of Noise Data.

unit variance. The spectrum of the noise is then compared with the spectrum of the model to see if they are reasonably close. Figure 3.5 shows the results of comparing the spectrums of the noise and the model using the same example as that used in Figure 3.4. This comparison shows that an 11^{th} order model performs reasonably well for this noise sequence, although a higher order model could possibly match the noise better.

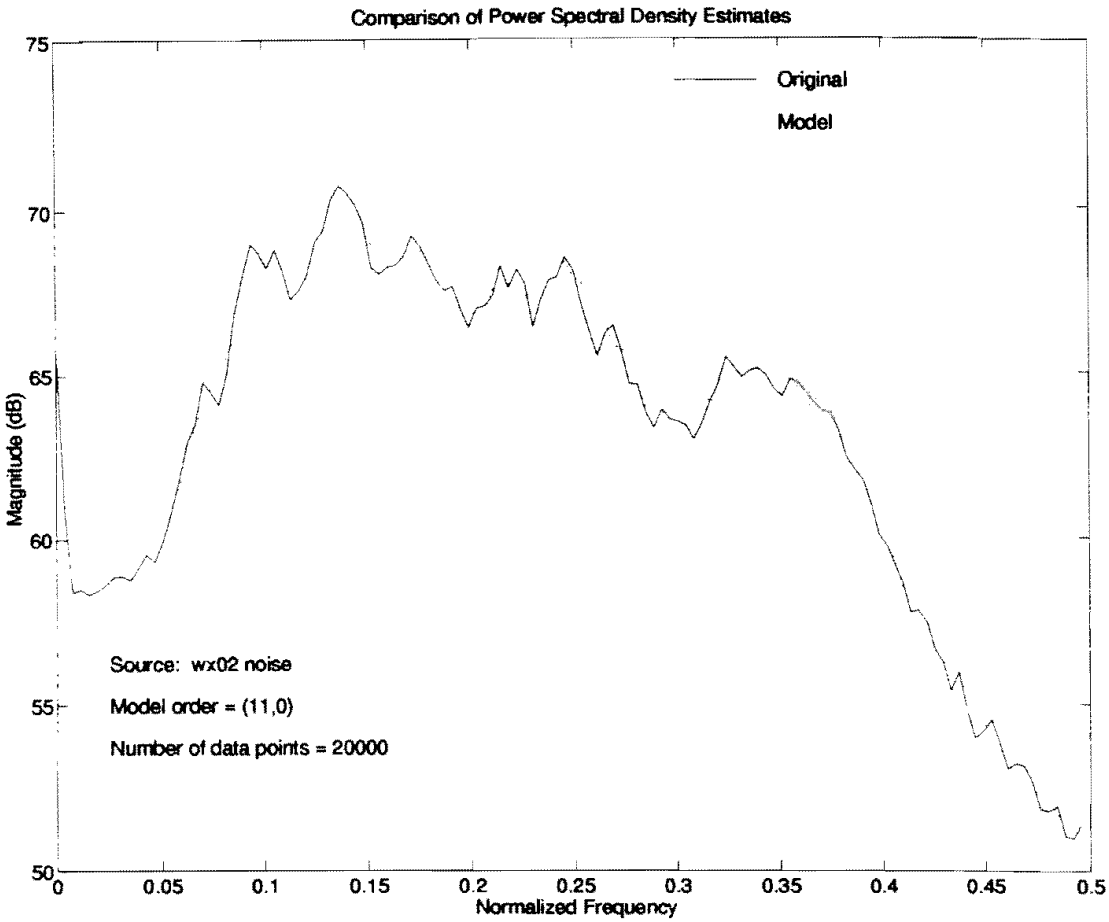

Figure 3.5: Example of Model Order Selection Based on Comparison of the Noise Spectrum and the Model Spectrum for Sequence *wx02* Using 20,000 Points of Noise Data.

4. Aural Evaluation

As a further means of testing, we can generate models of various orders and determine the lowest order model which gives the *best sounding* results. This test is performed by listening to the real noise and the modeled noise played back-to-back. The model is rejected if it is possible to hear the transition point between the noise and the model. Modeled noise which sounds indistinguishable from real noise can be generated using model orders typically lower than those predicted using either the theoretical

criteria or any of the other tests. The listening tests generally agree with the results obtained by comparing the noise and model spectrums, in that when it is possible to hear the difference between the noise and model then the spectra are also noticeably different. An 11^{th} order model was chosen for the above examples because this was the lowest model order for which it was not possible to hear the distinction between the real noise and the modeled noise. This demonstrates that aural evaluation is effective if a good sounding model is desired, but may not necessarily be the best if the most accurate model is required. The listening test and the prediction error filter output test turned out to give the most useful practical results.

IV. FILTERING AND RESULTS

An observed noisy transient signal can be thought of as a random process $x(n)$ which is related to another random process $s(n)$ which cannot be observed directly. If $x(n)$ is the transient with additive background noise, then $s(n)$ is an original transient signal free of noise. The goal of filtering is to *estimate* $s(n)$ from $x(n)$ for all n. The optimal filter which performs this estimation by minimizing the mean square error is known as the Wiener Filter. Its design is based on the *statistical* characteristics of the signal and the noise. If the noise is Gaussian, then the Wiener filter is the best filter (in the mean-square sense) for removing the noise. If the noise is not Gaussian, then the Wiener filter is the best *linear* filter for removing the noise although in general there may be a nonlinear filter which will perform better. [12]

The Wiener filter is usually designed for filtering *stationary* signals, which is a reasonable assumption for the noise but a poor assumption for the transient signal whose statistical characteristics change significantly over a short time. Accordingly we have extended the Wiener filter by considering a short-time approach which is effective for removing the noise from non-stationary signals, such as underwater transient signals.

A. WIENER FILTERING OF STATIONARY RANDOM SIGNALS

A signal in noise can be represented as

$$x(n) = s(n) + \eta(n) \tag{4.1}$$

where $x(n)$ is the received signal, $s(n)$ is the signal without noise, and $\eta(n)$ is the noise. It is assumed here that all quantities are real and have zero mean. When the signal

and noise are uncorrelated, as is typically the case for observed transient signals, the autocorrelation of the noisy signal is given by

$$R_x(l) = R_s(l) + R_\eta(l) \tag{4.2}$$

where $R_x(l)$ is the autocorrelation of the signal plus noise, $R_s(l)$ is the autocorrelation of the signal, and $R_\eta(l)$ is the autocorrelation of the noise. If a properly designed finite impulse response (FIR) filter is applied to the data then an estimate of the signal can be obtained from the convolution expression

$$\hat{s}(n) = \sum_{l=0}^{P-1} h(l)x(n-l) \tag{4.3}$$

where $h(n)$ is the impulse response and P is the order of the optimal filter. [12]

The Wiener filter, that minimizes the mean-square error, satisfies the Wiener-Hopf equation

$$\sum_{l=0}^{P-1} R_x(l-i)h(l) = R_{sx}(i); \quad i = 0, 1, \ldots, P-1 \tag{4.4}$$

where, since the signal and the noise are uncorrelated, the cross-correlation function between s and x is given by

$$R_{sx}(l) = R_s(l) \tag{4.5}$$

Using (4.5) in (4.4) and writing each of the P equations explicitly yields the matrix form of (4.4) as

$$\begin{bmatrix} R_x(0) & R_x(-1) & \cdots & R_x(1-P) \\ R_x(1) & R_x(0) & \cdots & R_x(2-P) \\ \vdots & \vdots & \ddots & \vdots \\ R_x(P-1) & R_x(P-2) & \cdots & R_x(0) \end{bmatrix} \begin{bmatrix} h(0) \\ h(1) \\ \vdots \\ h(P-1) \end{bmatrix} = \begin{bmatrix} R_s(0) \\ R_s(1) \\ \vdots \\ R_s(P-1) \end{bmatrix} \tag{4.6}$$

from which the filter weights $h(l)$ can be solved by simple matrix algebra.

B. SHORT-TIME APPROACH TO WIENER FILTERING

The Wiener filter described above works well for stationary signals, but several modifications are needed for non-stationary signals. In the short-time approach to Wiener

filtering the signal of interest is segmented into *short-time stationary* segments, where it is assumed that signal changes relatively slowly over small intervals. What constitutes short-time stationarity is largely subjective and depends on the signal. Speech, for example, is normally considered stationary over periods of 20 to 30 msec [24]. More slowly varying transients can be considered stationary over intervals of perhaps tenths of a second, while more quickly changing signals, such as impulsive signals, may only appear stationary over intervals of several microseconds.

1. Autocorrelation Estimates

In the short-time approach the autocorrelation function of the data is estimated for each segment, the filter weights are calculated for each segment, and finally each segment is filtered with the appropriate filter. Since the exact autocorrelation functions necessary to construct (4.6) are unknown, they must be estimated from the data. The *biased* estimate

$$\hat{R}_x(l) = \frac{1}{N_s} \sum_{n=0}^{N_s-1-l} x(n+l)x(n); \quad 0 \leq l < N_s \tag{4.7}$$

is used because it guarantees that the autocorrelation matrix in (4.6) will be positive definite and therefore nonsingular. Since the correlation function is symmetric, (4.7) needs only to be computed at zero and positive lag values. This estimator is asymptotically unbiased and consistent, which means that the estimate converges in probability to the actual correlation function as the number of samples tends to infinity. This implies that a compromise must be made in finding the best filter since stationarity requires the shortest possible segmentation while a good estimate of the autocorrelation requires the longest possible segments. [12]

Equation 4.6 requires the autocorrelation functions of both the noisy signal $x(n)$ and the noise-free signal $s(n)$. To estimate these correlation functions $R_\eta(l)$ can first be estimated by applying (4.7) to segments of the signal which contain only noise. Similarly,

$R_x(l)$ can be estimated for each segment containing the signal plus noise. $R_s(l)$ cannot be estimated directly, but it can be obtained by from (4.2) as

$$R_s(l) = R_x(l) - R_\eta(l) \tag{4.8}$$

2. Pre-Whitening

Since the estimates for $R_s(l)$ obtained by (4.8) can have some error, the filter for some segments of the signal can give poor results. Note that the estimate for $R_s(l)$ is not guaranteed to be positive definite even if the estimates for both $R_x(l)$ and $R_\eta(l)$ are positive definite. The estimate of $R_s(l)$ can be improved in practice by *pre-whitening* the signal because it reduces the problem of estimating the correlation function for the noise to that of estimating just a single parameter (the noise variance). Pre-whitening is accomplished by obtaining a good AR model for the noise using the method described in Chapter III, and then filtering the noisy data $x(n)$ with the prediction error filter (PEF) formed from the inverse model, as shown in Figure 4.1. If the AR model order was well

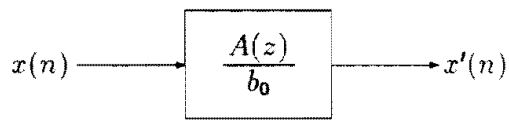

Figure 4.1: Prediction Error Filter.

chosen, then the output of the PEF $x'(n)$ will be white noise for noise only input. For sections of the original signal containing signal plus noise the output of the PEF will be a *colored* version of the original signal plus white noise, that is

$$x'(n) = s'(n) + \eta'(n) \tag{4.9}$$

where $\eta'(n)$ is Gaussian white noise. If the short-time filtering approach is applied to the output of the PEF rather than to the original signal, then $R'_\eta(l)$ can be assumed to be

the autocorrelation function of Gaussian white noise, which is simply an impulse with value equal to the estimated variance (ideally the noise variance will be 1.0). $R'_s(l)$ can then be estimated by simply subtracting this impulse from $R'_x(l)$. The advantage in this approach is that only the zero lag is affected by the subtraction whereas in the previous method all lag values were affected by the subtraction of $R_x(l)$ and $R_\eta(l)$. This new approach tends to reduce the effect of accumulated errors. For the sections of the signal containing only noise, ideally $R'_x(l) = R'_\eta(l)$ since $R'_s(l) = 0$. This should yield $h(n) = 0$ for $n = 0, 1, \ldots, P-1$, which means that the noise (which is the entire received signal) should be entirely removed from segments containing only noise.

It is important that not too much be subtracted from $R'_x(0)$ because this can cause the correlation function $R'_{s'}(l)$ to become indefinite and produce significant distortion. We chose to filter several segments of noise through the PEF and use the smallest of the resulting variances as the value to subtract from $R'_x(0)$. This conservative estimate decreases the chance of subtracting too much and lessens the chance that $R'_s(l)$ will become indefinite. In practice it was found that subtracting too little gives better results than subtracting too much.

Once the filter has been determined, the short-time Wiener filter is applied to the colored signal $x'(n)$ in order to produce an estimate of the clean colored signal $\hat{s}'(n)$. Then $\hat{s}'(n)$ is filtered with the AR model in order to obtain an estimate $\hat{s}(n)$ of the original signal. Figure 4.2 illustrates this process.

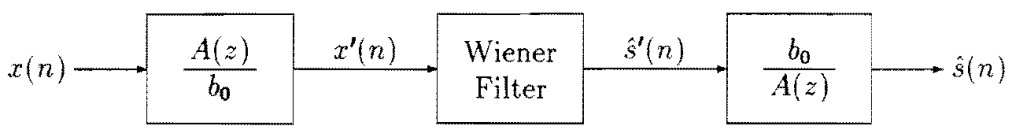

Figure 4.2: Pre-Whitening and the Short-Time Wiener Filter.

3. Smoothing Discontinuities

After all of the signal segments have been filtered the complete signal is constructed by joining all the segments into one signal. Since each segment is filtered with a slightly different filter, some smoothing techniques must be applied so that the differences at the segment boundaries do not become noticeable. These differences produce a distortion that is mainly from the noise that remains in the signal after filtering, and is most noticeable in the segments containing more noise than signal.

a. Initializing the Filter Conditions

One technique to help smooth the discontinuities is to use the final conditions from the filter of one segment as the initial conditions of the filter for the succeeding segment. If the segment lengths provide a reasonably good approximation of stationarity, then the filter from one segment should not be significantly different from the filters on either side. Therefore the final conditions of one filter should give a fairly good approximation of what the initial conditions should be in the next filter. This technique thus reduces the effects of an unwanted transient response caused by the lack of appropriate initial conditions.

b. Overlap-averaging

Another way to minimize the effects of the boundary discontinuities is prevent any filtered segment from beginning or ending abruptly. One way to accomplish this is as follows. Each filtered segment is weighted by a triangular window, as illustrated in Figure 4.3 (a) and (b), to form a windowed sequence $\hat{s}_1(n)$. Then the original signal is resegmented as shown in Figure 4.3 (c) and windowed, as shown in Figure 4.3 (d), to form another windowed sequence $\hat{s}_2(n)$. The two windowed sequences are then added to form the complete signal $\hat{s}(n)$ as shown in Figure 4.3 (e). The effect of adding $\hat{s}_1(n)$ and

$\hat{s}_2(n)$ is to continually phase out one segment while phasing in the next, thus smoothing the discontinuities between segments.

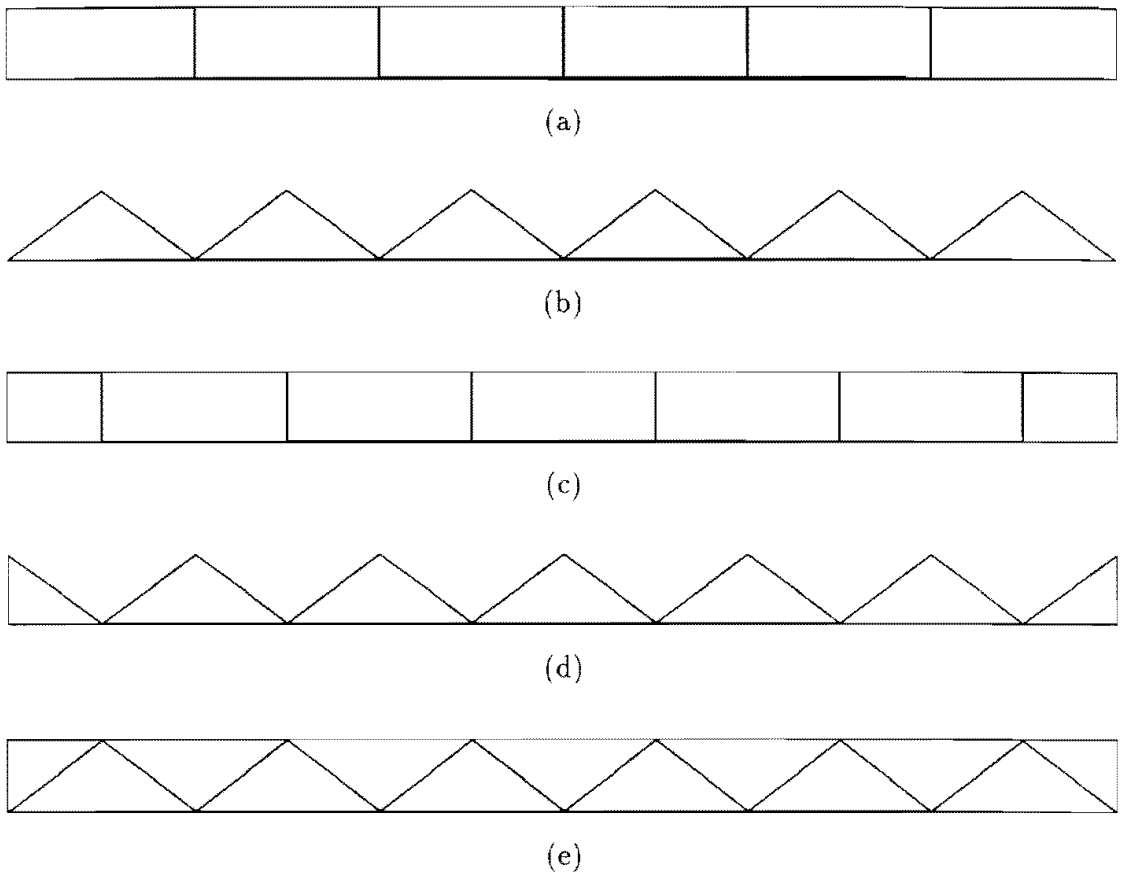

Figure 4.3: Overlap-Averaging Technique for Smoothing Boundary Discontinuities. (a) Segmented signal. (b) Amplitude scaling for the segmented signal. (c) Re-segmented signal. (d) Amplitude scaling for the re-segmented signal. (e) Signal smoothed by overlap-averaging.

4. Forward-Backward Filtering

The FIR filtering process described above induces a linear phase shift in the filtered signal. This phase shift can be compensated for by filtering in the forward *and* backward directions. For the process described in the previous section this is accomplished

by filtering each segment in the forward direction using the final condition of each filter as the initial condition for the next filter. After filtering each segment, the process is reversed. Beginning with the final filter segment the reversal of each filtered segment is then filtered again, with the same filter used in the forward direction.

5. Filter Parameters

Four parameters must be chosen in order to obtain effective filtering. The most important consideration is the segment length of the original signal, which should be as many points as possible. Ideally, the segments should each contain 1000 or more points of data because the accuracy of the autocorrelation estimate improves with the number of points used. This is not always possible due to the competing requirement for stationarity. The second consideration is the order of the FIR Wiener filter. High order filters work well if the autocorrelation function is estimated well, as with data which changes slowly and can be segmented into long segments. Low order filters give better results for data which changes quickly and therefore requires the use of smaller segments. Finally, the noise must be modeled well which means that a representative segment of the noise must be used and an appropriate model order for the noise must be chosen, as described in Chapter III.

C. RESULTS

1. Graphical Results

Figures 4.4 through 4.7 show the results of filtering several transient signals. The magnitude scale for each signal represents the integer value of the output of the analog-to-digital converter, not the actual strength of the signal in the ocean (for example, 16-bit quantization yields a magnitude scale from -32,768 to +32,767). Figure 4.4 is data from a killer whale song. The sampling rate is 22.05 kHz, the segment length is

50 msec (1102 points), the filter order is 50, and the noise was modeled with a 35^{th} order AR model using 12,000 points of data. Since the signal had a high sampling rate it was possible to segment the data into long segments and still maintain a reasonable approximation of stationarity, allowing the use a high order filter. A significant amount of noise was removed from filtered signal with little added distortion. Figure 4.5 is data from a porpoise whistle. The sampling rate is 12.5 kHz, the segment length is 200 msec (2500 points), the filter order is 50, and the noise was modeled with a 35^{th} order AR model using 20,000 points of data. The sampling rate was slower than that used for Figure 4.4, but the signal changed much more slowly, allowing for longer segmentation and a high order filter. The filtering process was particularly effective for this transient, as the noise was nearly entirely removed from the signal with almost no added distortion. Figure 4.6 is data from a stochastically generated transient. The sampling rate and time are not mentioned here in order to avoid revealing the source. The segment length is 500 points, the filter order is 10, and the noise was modeled with a 35^{th} order AR model using 20,000 points of data. The characteristics of the signal changed quickly with respect to the sampling rate, which necessitated the short segment lengths and the low order filter. Much of the original noise was removed, but the distortion was more noticeable than with the two previous examples. Figure 4.7 is data from an impulsive source. The sampling rate and time are also not mentioned. The segment length is 500 points, the filter order is 20, and the noise was modeled with a 35^{th} order AR model using 20,000 points of data. A short segment length and low filter order were similarly required for this transient since its characteristics changed quickly with respect to the sampling rate. This was generally true for all of the transients we tested which were impulsively generated.

The amount of distortion caused by the filtering process depends, in general, on how quickly the signal changes with respect to the sampling rate. The obvious implication is that the short-time Wiener filter should be more effective with signals sampled at very

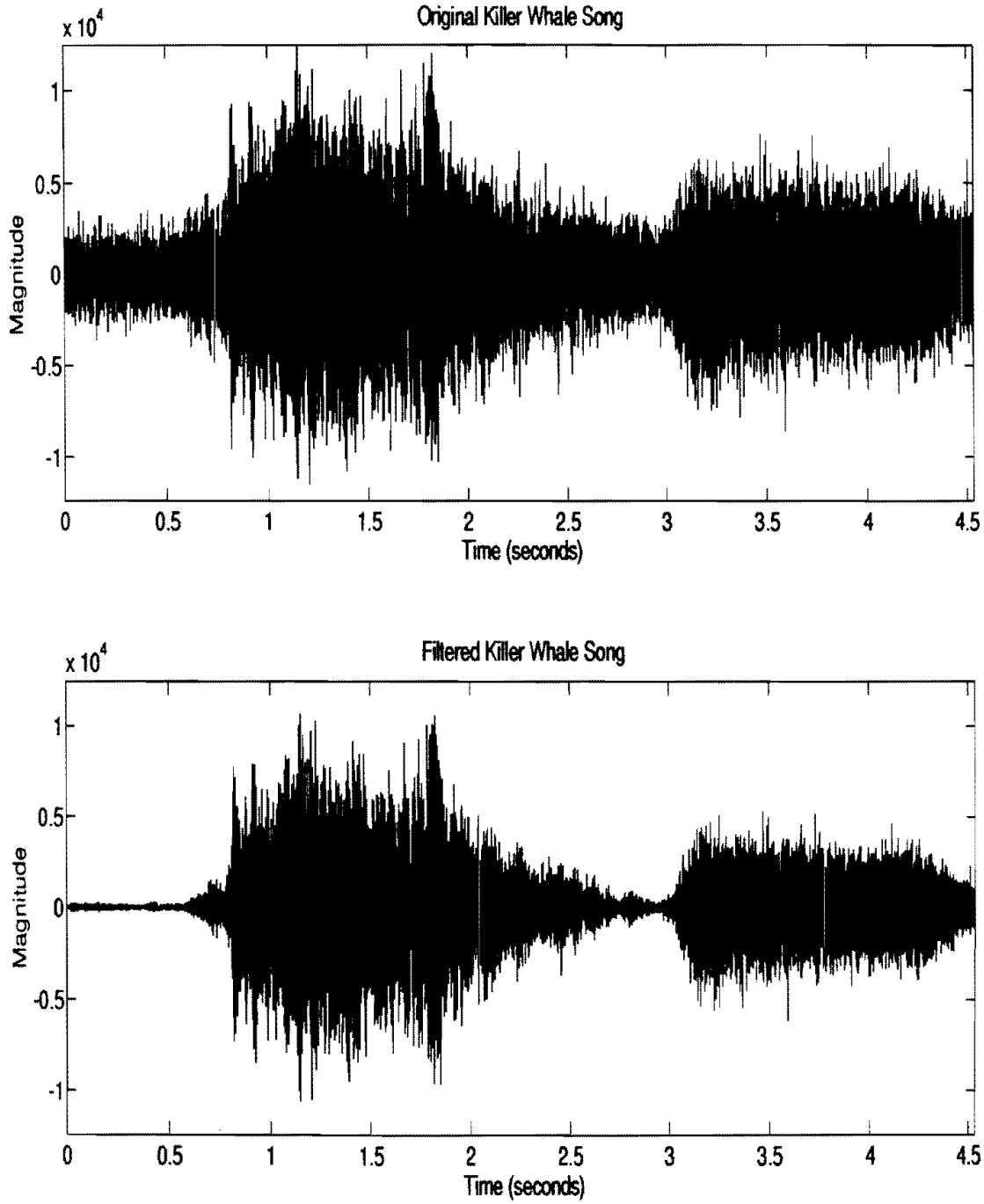

Figure 4.4: Results of Filtering a Transient Signal Generated by a Killer Whale Song (Sequence *orca*).

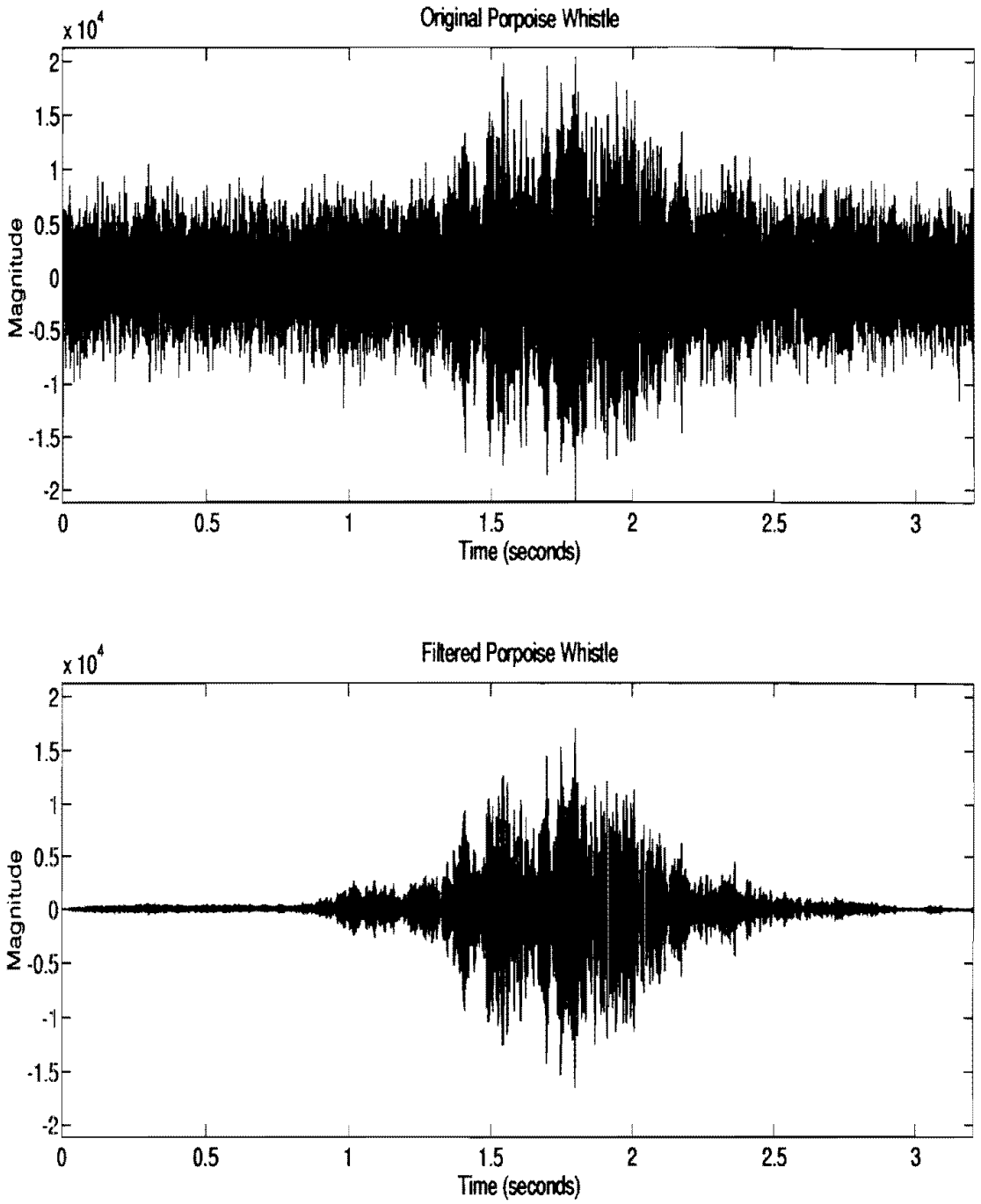

Figure 4.5: Results of Filtering a Transient Signal Generated by a Porpoise Whistle (Sequence *bio-2385*).

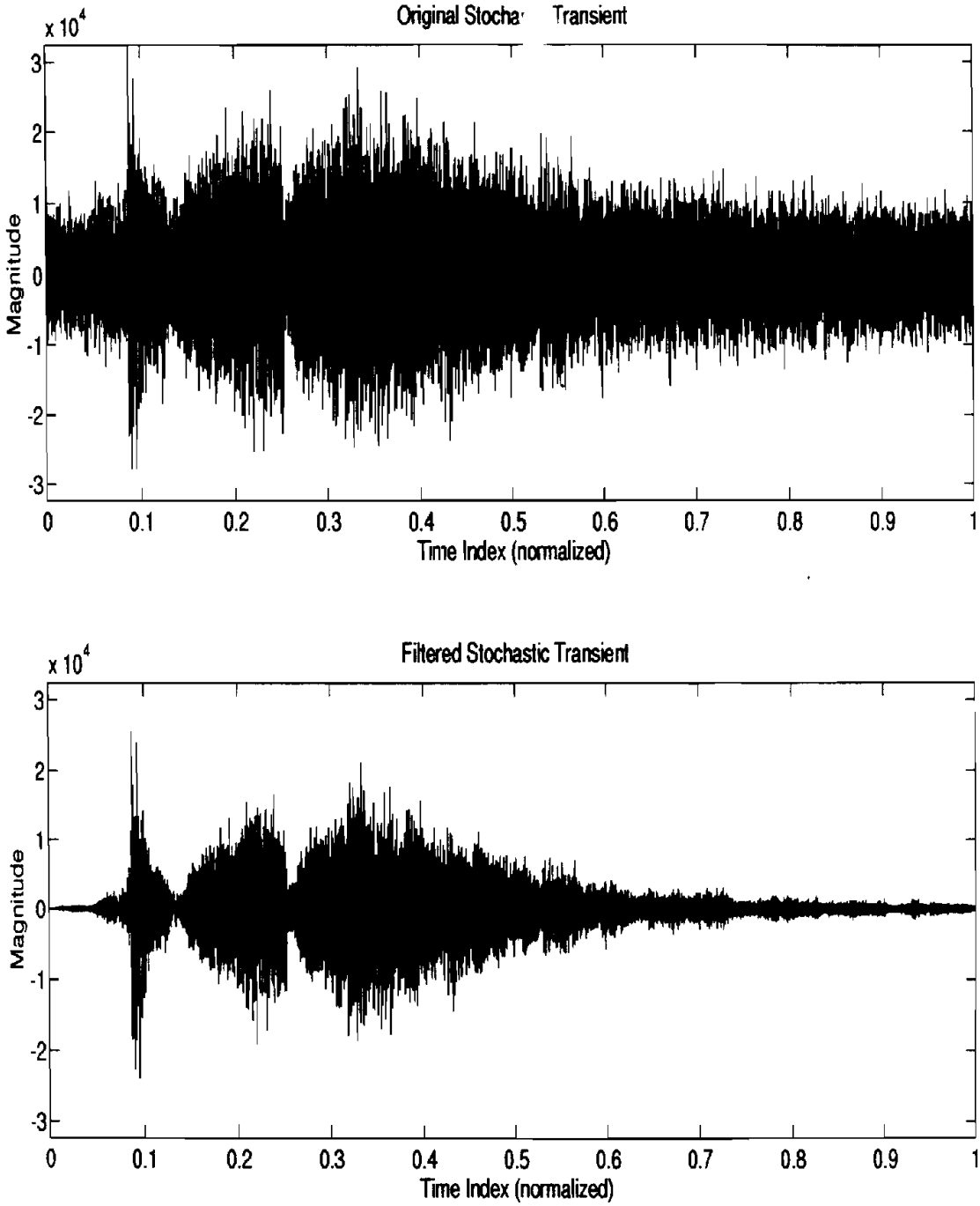

Figure 4.6: Results of Filtering a Stochastically Generated Transient Signal.

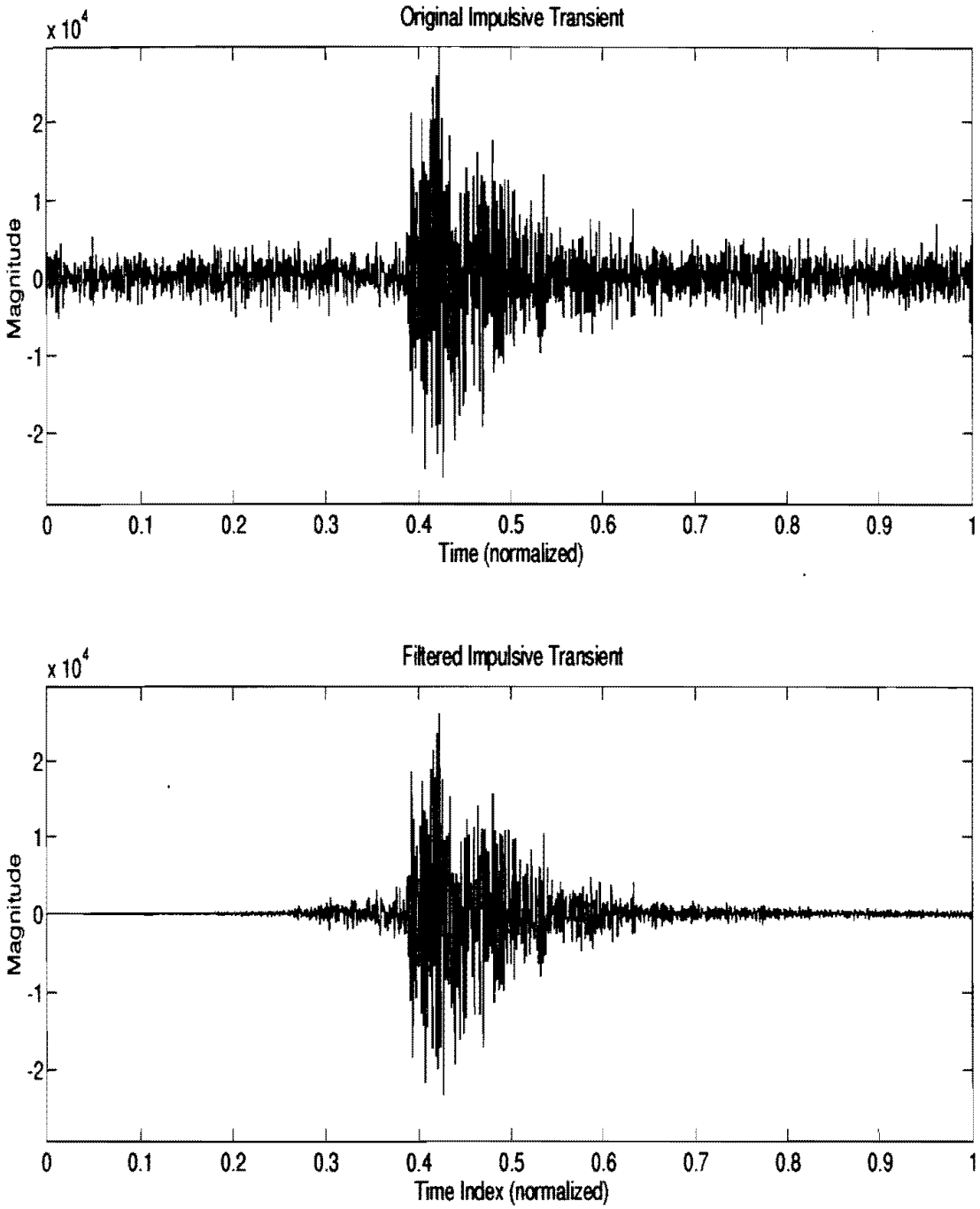

Figure 4.7: Results of Filtering an Impulsive Transient Signal.

high sampling rates. If the filtered signals are to have synthetically generated noise added to them, as described in the next section, then the distortion is not a significant problem since the added noise typically hides small amounts of distortion.

2. Results of Aural Testing

A subjective listening experiment was developed to see if human listeners are able to distinguish between real underwater transient signals and synthetically generated transient signals produced by the technique described in this thesis. The goal of this experiment was to demonstrate that by effective use of noise modeling and noise removal it is possible to generate synthetic transient signals which are indistinguishable from real transient signals. The experiment consisted of two parts and twelve individual tests. Part one contained tests one through eight, which each consisted of listening to three signals: two real transient signals in noise and one synthetically generated transient signal in synthetically generated noise. In Part one each listener was asked to identify the one synthetically generated signal for each of the tests. Table 4.1 indicates how the signals were generated. The synthetic signals in tests 1, 5, and 7 were generated without first

Test Number	Signal A	Signal B	Signal C
1*	real *wx01*	synthetic *wx01*	real *wx02*
2	synthetic *wx01*	real *wx11*	real *wx01*
3	real *wx02*	synthetic *wx03*	real *wx03*
4	synthetic *qx01*	real *qx02*	real *qx03*
5*	real *qx01*	real *qx02*	synthetic *qx03*
6	real *qx01*	synthetic *qx02*	real *qx03*
7*	real *porpoise*	synthetic *porpoise*	real *porpoise*
8	synthetic *porpoise*	real *porpoise*	real *porpoise*

TABLE 4.1: TESTS COMPRISING PART ONE OF THE SUBJECTIVE LISTENING EXPERIMENT. The * indicates the tests with signals which were synthesized without first removing the noise. The *wx* and *qx* signals are as described in Chapter II.

removing the noise. The rest of the synthetic signals were generated by first removing the noise, then synthesizing the transient, and finally adding synthesized noise at an appropriate signal to noise ratio. Synthesizing some signals without first removing the noise was intended to show the that noise removal and modeling improves the "realness" of the synthetic signals.

Part two contained tests nine through twelve, which each consist of three real transient signals in noise: one transient signal which is unaltered and two transient signals which have the original noise replaced by synthetically generated noise. In Part two each listener was asked to identify the signal which was unaltered. Table 4.2 indicates how the signals in Part two were generated.

Test Number	Signal A	Signal B	Signal C
9	original *wx01* noise from *qx03*	filtered *wx01* with noise from *orca*	filtered *wx01* with
10	filtered *porpoise* with noise from *wx02*	filtered *porpoise* with noise from *orca*	original *porpoise*
11	filtered *qx03* with noise from *wx02*	original *qx03*	filtered *qx03* with noise from *wx02*
12	filtered *porpoise* with noise from *porpoise*	original *porpoise*	filtered *porpoise* with noise from *porpoise*

TABLE 4.2: TESTS COMPRISING PART TWO OF THE SUBJECTIVE LISTENING EXPERIMENT.

All of the signals in tests 1, 2, 3, and 9 were generated from a common type of source and noise background. Similarly, the signals in tests 4, 5, 6, and 11 are all from the same type of source. The signals in tests 7, 8, 10, and 12 are all porpoise whistles embedded in noise. Placing signals of the same class in each test was intended to give the listeners the advantage of being able to compare the synthetic signals with real signals, and possibly improve their scores. The tests were also designed to deceive the listeners by selecting the signals in such a way that they are drawn to false clues, such as signal

to noise ratios or other characteristics. For example, tests 2 and 3 each consist of two real signals which sound different from one another along with a synthetic signal which sounds very similar to one of the real signals; in test 12 the signal to noise ratio is varied. This "trickery" is included in order to demonstrate that the listener is forced to resort to clues which have nothing to do with whether or not the signal is real, thereby showing the effectiveness of the synthesis. The synthetic signals for the tests were all generated using the iterative Prony method [6], with a segment length of forty samples and a model order of twelve. The synthetic noise in each test was generated with a 35^{th} order AR model of various noise sources. The filtered signals were obtained by using short-time Wiener filtering with the filter parameters chosen to give the best sounding signals.

Of the 12 people who participated in the test, five are submarine officers, four are professors at the Naval Postgraduate School with extensive signal synthesis experience (one is also a former submarine officer), two are Navy sonar operators, and one is a P-3C (an anti-submarine warfare aircraft) Tactical Action Coordinator. Table 4.3 lists the results of the first part of the subjective listening test. The numbers in the table indicate how many "votes" each signal received, with the correct choice indicated by the boxes.

Test Number	Signal A	Signal B	Signal C
1*	0	**11**	1
2	**4**	6	2
3	11	**1**	0
4	**4**	6	2
5*	1	0	**11**
6	3	**1**	8
7*	2	**9**	1
8	**6**	1	5

TABLE 4.3: RESULTS FROM PART ONE OF THE SUBJECTIVE LISTENING EXPERIMENT. The * indicates the tests with signals which were synthesized without first removing the noise.

Again the * indicates the signals which were synthesized without taking the effects of the noise into account. Notice that these tests (marked with an *) received the most correct votes, showing that traditional synthesis techniques can yield poor models when background noise is present. With the noise taken into account in the synthesis process and with well designed models the participants could not consistently tell the difference between real and synthesized signals and frequently made wrong choices. In some cases nearly every participant was deceived by the data (see the results from test 3 and 6).

Table 4.4 lists the results of the second part of the subjective listening Experiment. Once again the numbers in the table indicate how many "votes" each signal

Test Number	Signal A	Signal B	Signal C
9	**9**	0	3
10	6	1	**5**
11	8	**3**	1
12	5	**4**	3

TABLE 4.4: RESULTS FROM PART TWO OF THE SUBJECTIVE LISTENING EXPERIMENT.

received, with the correct choice indicated by the boxes. The results of this part show that it is possible to change the noise background of a signal (either by replacing the original noise with a different type of noise or by replacing the original noise by the same type of noise but with a different SNR) without destroying its "authenticity." In all but one of the tests, listeners were unable to consistently identify any of the original signals.

It was expected that each listener would correctly choose the signals which were synthesized without noise removal, yielding a potential minimum score or three. It was further expected that, given good signal synthesis, each listener would randomly choose the correct answers from the remaining nine tests, giving an expected score of three out of the remaining nine. This yields an expected score of six. An average score higher than

six would indicate that the signals were not convincingly real. An average score of less than six would indicate that the listeners were drawn to false clues, thereby verifying the effectiveness of the synthesis. The number of correct scores for the twelve tests ranged from one to ten, with the average number of correct answers being 5.5.

Qualitatively, all of the participants expressed their difficulty in selecting the correct choice. In many cases it came down to their "best guess." All of the participants noted that the signals synthesized by removing the noise prior to modeling were superior to those synthesized without noise removal.

V. CONCLUSIONS

A. DISCUSSION OF RESULTS

Synthesis of underwater transient signals can be significantly improved if the ambient ocean noise is taken into account in the synthesis process. The noise, which is typically Gaussian, can be filtered from the signal using linear techniques. In particular, we demonstrated that the Wiener filter, which is an optimal linear filter, can be effectively modified for use in a "short-time" manner in order to filter stationary noise from a transient signal. In order to make the short-time Wiener filter perform satisfactorily a number of techniques were required to reduce the effects of distortion caused by the filtering. The distortion is mainly due to the inability to obtain exact estimates of the autocorrelation function for each of the short-time segments used in the short-time Wiener filter while at the same time segmenting the data in short enough segments to obtain a good approximation of stationarity. We found that in most cases a reasonable balance can be obtained which yields useful results.

Finding a good model of the noise is important for at least two reasons. First, it is necessary in order to remove noise from a real signal prior to analysis and synthesis. Secondly, high quality noise models are essential to the formation of high quality synthetic signals. We found that the AR model gave the best results in terms of simplicity of computation, usefulness in the application of pre-whitening, and the best "sounding" noise.

B. SUGGESTIONS FOR FURTHER STUDY

The results from this thesis lead to several interesting possibilities for future research. These possibilities include:

1. Training and testing artificial neural networks. We demonstrated that human listeners are typically unable to tell the difference between real signals and synthetically generated signals when the noise is taken into account in the synthesis process. However, this may not necessarily be true for artificial neural networks, as the filtering process may introduce false clues unnoticeable to humans which could adversely affect training of an automatic classifier. The methods described in this thesis should be applied to artificial neural networks to determine if the synthesis is as effective as it is for human classifiers.

2. Real-time implementation. The short-time Wiener filter is non-causal and therefore not strictly applicable to *real-time* processing. It could however potentially be modified to work in a *nearly* real-time manner by applying the short-time method described in this thesis to segments of data which are perhaps as long as several seconds. For example, the filter could be used to remove the noise from two-second segments of data. Each two-second segment would then be segmented into sequences of perhaps 50 msec and filtered as described in this thesis. The output of such a filter would be delayed by two seconds plus the processing time, however it could potentially allow a human classifier to work at nearly real-time in a less noisy environment.

3. Nonstationary noise models. The noise models we developed are stationary. This is a good approximation for short duration signals but may be inadequate for longer synthetic signals. Time-varying models should be examined since they may further improve the authenticity of synthetically generated signals.

4. Non-linear filtering and modeling. Finally, since the data tested to have a Gaussian distribution, the use of linear techniques is justified. Non-linear methods however

could yield better results in the presence of known non-Gaussian noise sources. These would have to be examined on a case-by-case basis

LIST OF REFERENCES

[1] W. Chang, B. Bosworth, and G. C. Carter, "On using back propagation neural networks to separate single echoes from multiple echoes," In *1993 IEEE Int. Conf. Acoust. Speech and Signal Processing*, volume 1, pages 265–268, April 1993.

[2] J. R. Pierce and Jr. E. E. David, *Man's World of Sound*, Doubleday & Company, Inc., Garden City, New York, 1958.

[3] M. Loeb, *Noise and Human Efficiency*, John Wiley & Sons, Ltd., New York, 1986.

[4] T. P. Johnson, "ARMA modeling methods for acoustic signals," Master's thesis, Naval Postgraduate School, Monterey, California, March 1992.

[5] G. L. May, "Pole-zero modeling of transient waveforms: A comparison of methods with application to acoustic signals," Master's thesis, Naval Postgraduate School, Monterey, California, March 1991.

[6] G. K. Pfeifer, "Transient data synthesis: A deterministic approach," Master's thesis, Naval Postgraduate School, Monterey, California, December 1993.

[7] R. J. Urick, *Ambient Noise in the Sea*, Peninsula Publishing, Los Altos, California, 1986.

[8] R. J. Urick, *Principles of Underwater Sound, 3rd edition*, McGraw-Hill, Inc., New York, 1983.

[9] P. Z. Peebles, Jr., *Probability, Random Variables, and Random Signal Principles, 2nd edition*, McGraw-Hill, Inc., New York, 1987.

[10] F. W. Machell and C. S. Penrod, "Probability density functions of ocean acoustic noise processes," In E. J. Wegman and J. G. Smith, editors, *Statistical Signal Processing*, Marcel Dekker, Inc., New York, 1984.

[11] F. W. Machell, C. S. Penrod, and G. E. Ellis, "Statistical characteristics of ocean acoustic noise processes," In E. J. Wegman, S. C. Schwartz, and J. B. Thomas, editors, *Topics in Non-Gaussian Signal Processing*, Springer-Verlag, New York, 1989.

[12] C. W. Therrien, *Discrete Random Signals and Statistical Signal Processing*, Prentice Hall, Inc., Englewood Cliffs, New Jersey, 1992.

[13] The MathWorks, Inc., Natick, Massachusetts, *Matlab Reference Guide*, August 1992.

[14] T. C. Fry, *Probability and Its Engineering Uses, 2nd edition*, D. Van Nostrand Company, Princeton, New Jersey, 1965.

[15] E. R. Dougherty, *Probability and Statistics for the Engineering, Computing, and Physical Sciences*, Prentice Hall, Inc., Englewood Cliffs, New Jersey, 1990.

[16] L. J. Bain and M. Engelhardt, *Introduction to Probability and Mathematical Statistics*, Duxbury Press, Boston, Massachusetts, 1987.

[17] A. Swami, J. M. Mendel, and C. L. Nikias, *Hi-Spec Toolbox User's Guide*, United Signals and Systems, Inc., 1993.

[18] F. C. Mills, *Statistical Methods, revised*, Henry Holt and Company, Inc., New York, 1938.

[19] A. Papoulis, *Probability and Statistics*, Prentice Hall, Inc., Englewood Cliffs, New Jersey, 1990.

[20] M. J. Hinnich, "Testing for Gaussianity and linearity of a stationary time signal," *Journal of Time Series Analysis*, 3(3):169–176, 1982.

[21] A. T. Erdem and A. M. Tekalp, "On the measure of the set of factorizable polynomial bispectra," *IEEE Transactions on Acoustics, Speech, and Signal Processing*, 38(9):1637–1639, September 1990.

[22] S. M. Kay, *Modern Spectral Estimation: Theory and Application*, Prentice Hall, Inc., Englewood Cliffs, New Jersey, 1988.

[23] S. L. Marple, Jr., *Digital Spectral Analysis with Applications*, Prentice Hall, Inc., Englewood Cliffs, New Jersey, 1987.

[24] L. R. Rabiner and R. W. Schafer, *Digital Processing of Speech Signals*, Prentice Hall, Inc., Englewood Cliffs, New Jersey, 1978.

INITIAL DISTRIBUTION LIST

1.	Defense Technical Information Center Cameron Station Alexandria, VA 22304–6145	2
2.	Dudley Knox Library, Code 52 Naval Postgraduate School Monterey, CA 93943–5101	2
3.	Chairman, Code EC Department of Electrical and Computer Engineering Naval Postgraduate School Monterey, CA 93943–5121	1
4.	Prof. Charles W. Therrien, Code EC/Ti Department of Electrical and Computer Engineering Naval Postgraduate School Monterey, CA 93943–5121	2
5.	Prof. Ralph Hippenstiel, Code EC/Hi Department of Electrical and Computer Engineering Naval Postgraduate School Monterey, CA 93943–5121	1
6.	Prof. James H. Miller, Code EC/Mr Department of Electrical and Computer Engineering Naval Postgraduate School Monterey, CA 93943–5121	1
7.	Prof. James Eagle, Code OR/Er Undersea Warfare Academics Group Naval Postgraduate School Monterey, CA 93943–5219	1
8.	Mr. Steve Greineder, Code 2121 Naval Undersea Warfare Center New London, CT 06320–5594	1

9.	Mr. Tod Luginbuhl Naval Undersea Warfare Center New London, CT 06320–5594	1
10.	Mr. Michael Gouzie, Code 2121 Naval Undersea Warfare Center New London, CT 06320–5594	2
11.	Commander, Naval Sea Systems Command Attn: Cdr. Thomas Mason (Code 06UR) Naval Sea Systems Command Headquarters Washington, D.C. 20362–5101	1
12.	Commander, Naval Air Systems Command Attn: Mr. Earl Benson (PMA 264, Room 740, JP–1) Naval Air Systems Command Headquarters Washington, D.C. 20361–5460	1
13.	Defense Advanced Research Projects Agency Attn: Mr. Paul Rosenstrach Suite 600 1555 Wilson Blvd. Arlington, VA 22209	1
14.	Mr. Lou Griffith Code 7304 NCCOSC, RDT & E Division San Diego, CA 92152–5000	1
15.	LT Kenneth L. Frack, Jr., USN 3133 S.E. 158th Ave. Portland, OR 97236	1